

Results from a transport scheme intercomparison and design of a new non-linear transport-chemistry test



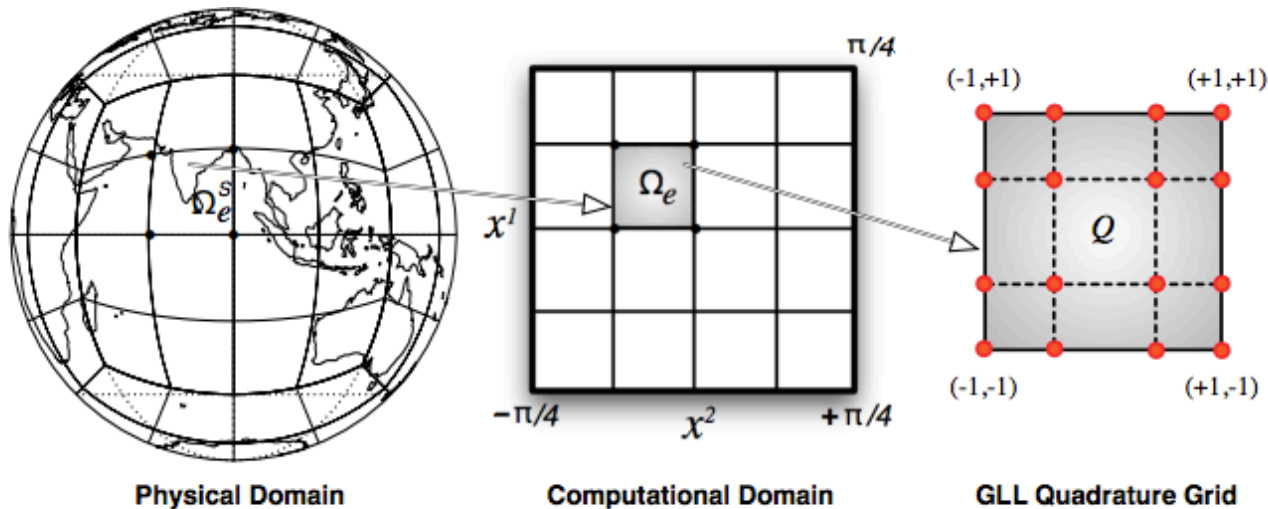
**Peter Hjort Lauritzen (NCAR), J.-F. Lamarque (NCAR),
M.J. Prather (U.C. Irvine), W.C. Skamarock (NCAR) and
M.A. Taylor (SNL)**

**Seminar at Max-Planck-Institut für Meteorologie (MPI-M)
July 23, 2013**

Some things that I will NOT talk about

1. Release of Spectral-Element (SE) dynamical core in CAM:

SE 1 degree CAM5 “AMIP” configuration are now scientifically supported!
(SE supports mesh-refinement)



SE supports
mesh-refinement

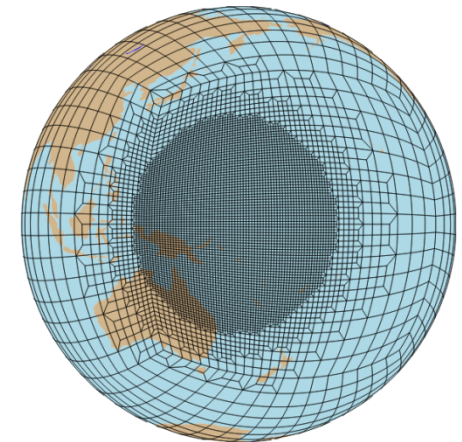


Fig. 9.22 A schematic diagram showing the mapping between each spherical tile (element) Ω_e^S of the physical domain (cubed-sphere) \mathcal{S} onto a planar element Ω_e on the computational domain \mathcal{C} (cube). For a DG discretization each element on the cube is further mapped onto a unique reference element Q , which is defined by the Gauss-Lobatto-Legendre (GLL) quadrature points. The horizontal discretization of the HOMME dynamical cores relies on this grid system.

Figure from Nair et al. (2011)

Some things that I will NOT talk about

1. Release of Spectral-Element (SE) dynamical core in CAM:

SE 1 degree CAM5 “AMIP” configuration are now scientifically supported!
(SE supports mesh-refinement)

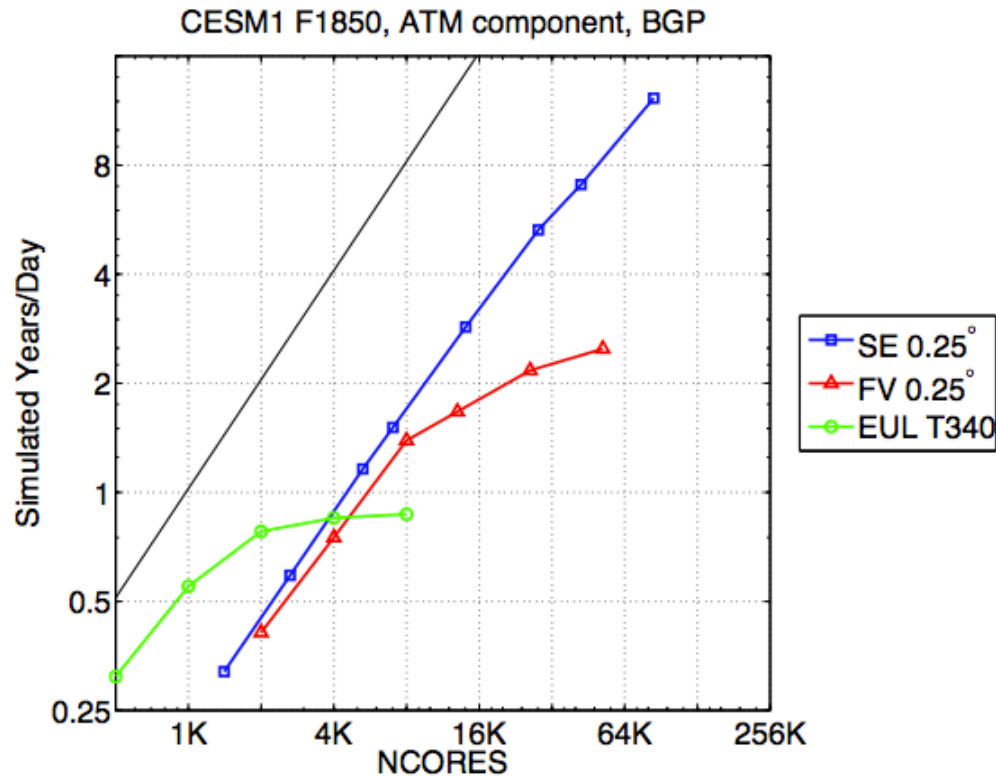


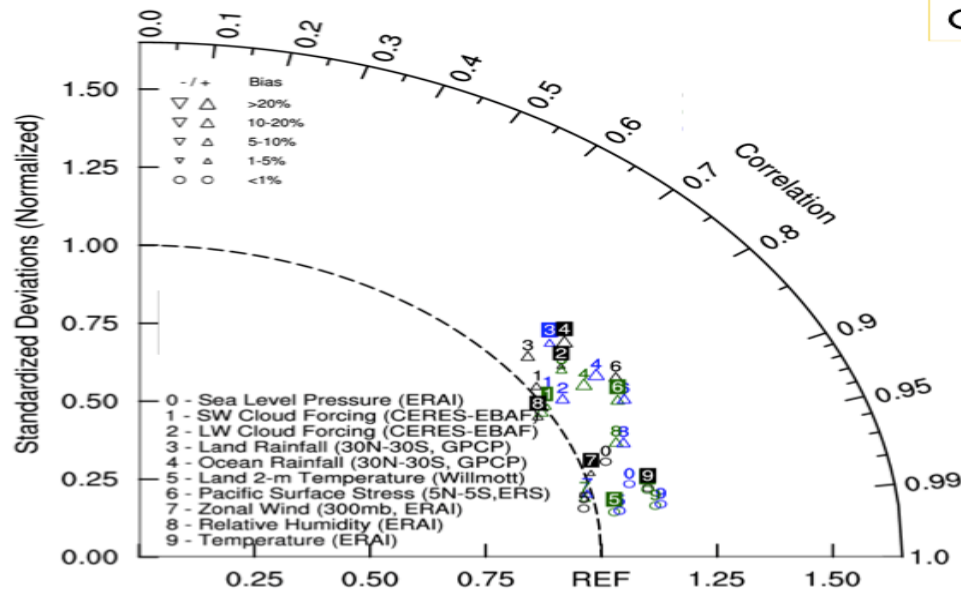
Figure from Dennis et al. (2012)

Some things that I will NOT talk about

1. Release of Spectral-Element (SE) dynamical core in CAM:

SE 1 degree CAM5 “AMIP” configuration are now scientifically supported!

AMIP runs: Taylor diagram



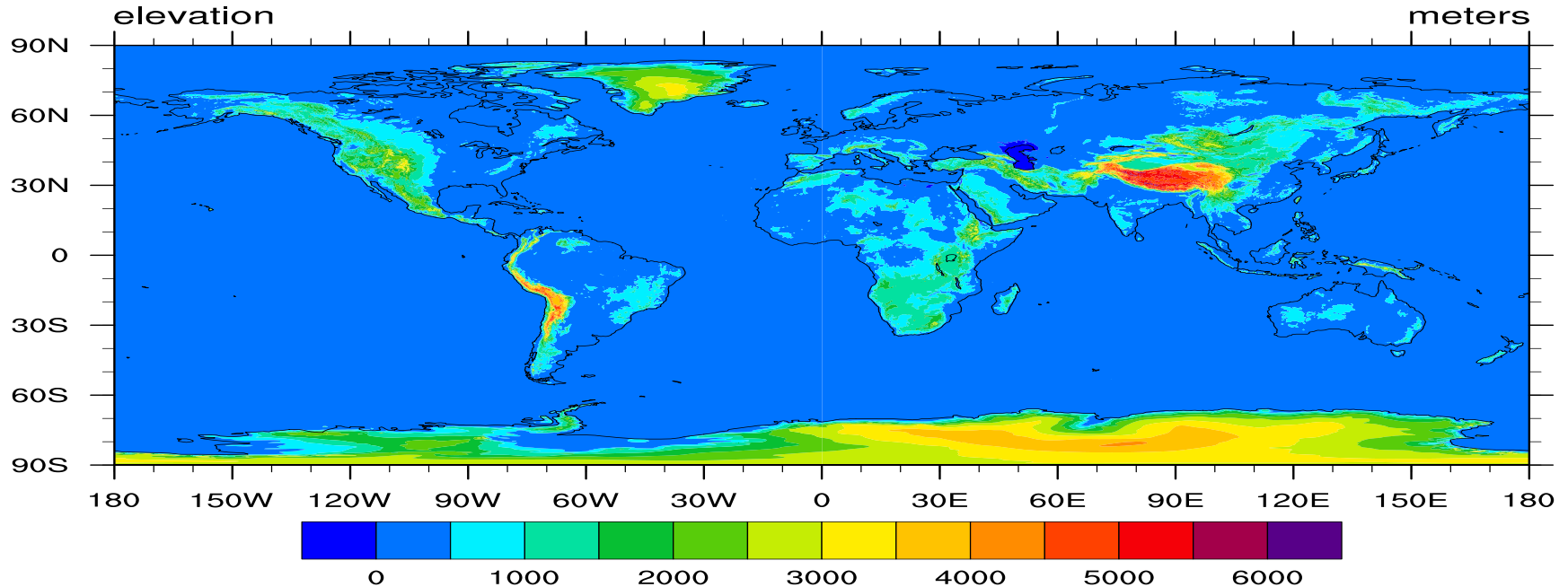
	RMSE	Bias
CAM-FV	0.88	1.21
CAM-SE	0.83	1.19

- CCSM3.5
- CAM-FV (1deg)
- CAM-SE (ne30)

Some things that I will NOT talk about

2. New topography generation software for unstructured grids with consistent computation of sub-grid-scale variables (for turbulent mountain stress & orographic gravity wave drag): released with CAM5.3

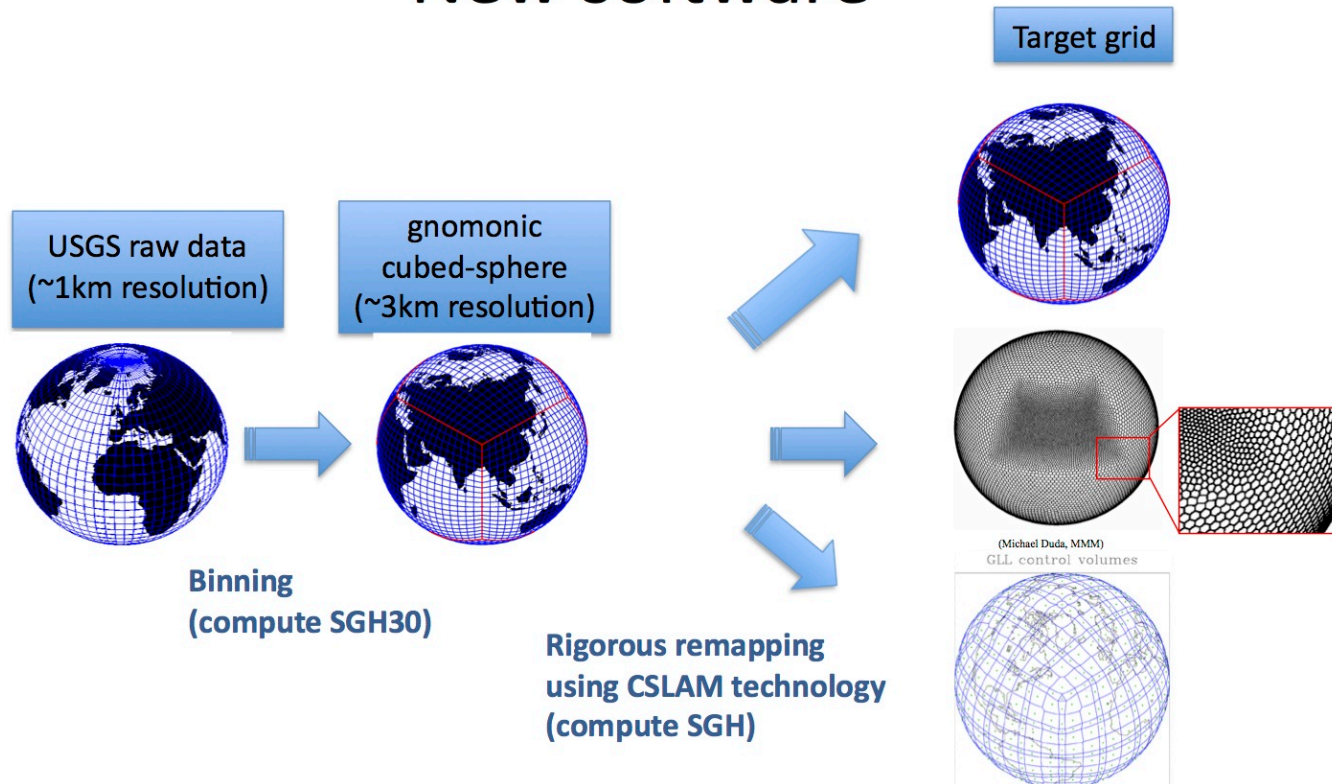
USGS raw data



Some things that I will NOT talk about

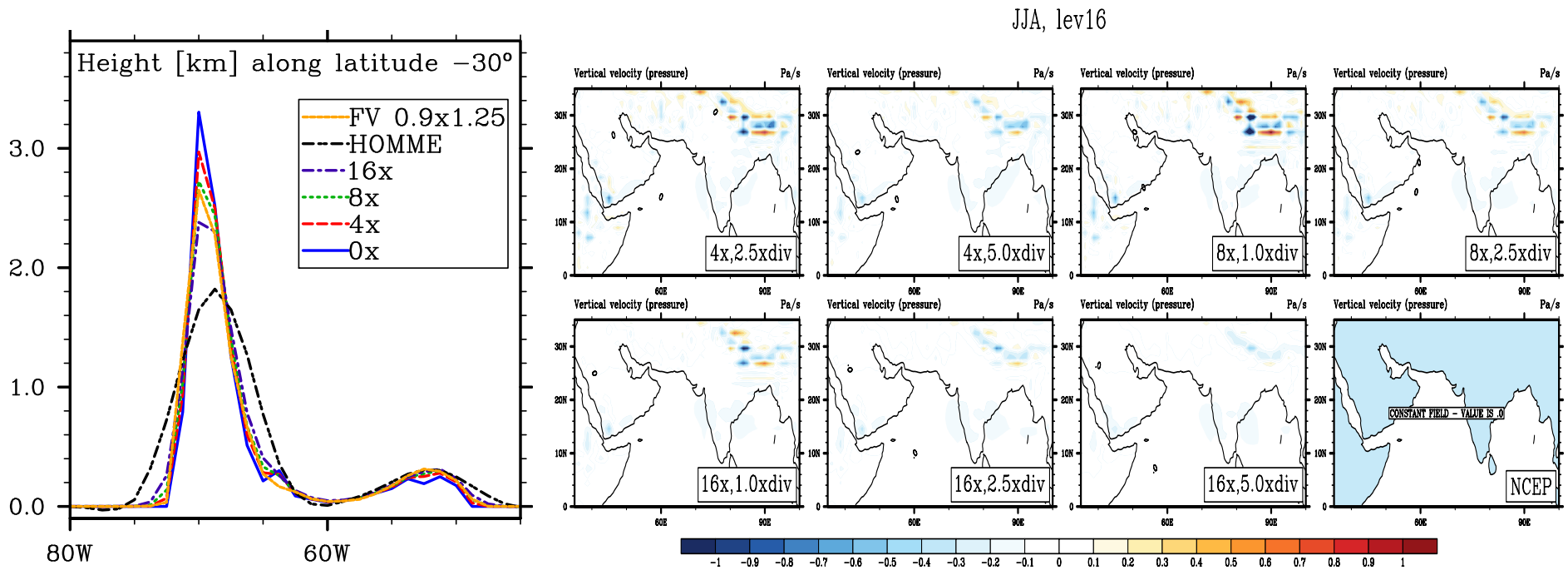
2. New topography generation software for unstructured grids with consistent computation of sub-grid-scale variables (for turbulent mountain stress & orographic gravity wave drag): released with CAM5.3

New software



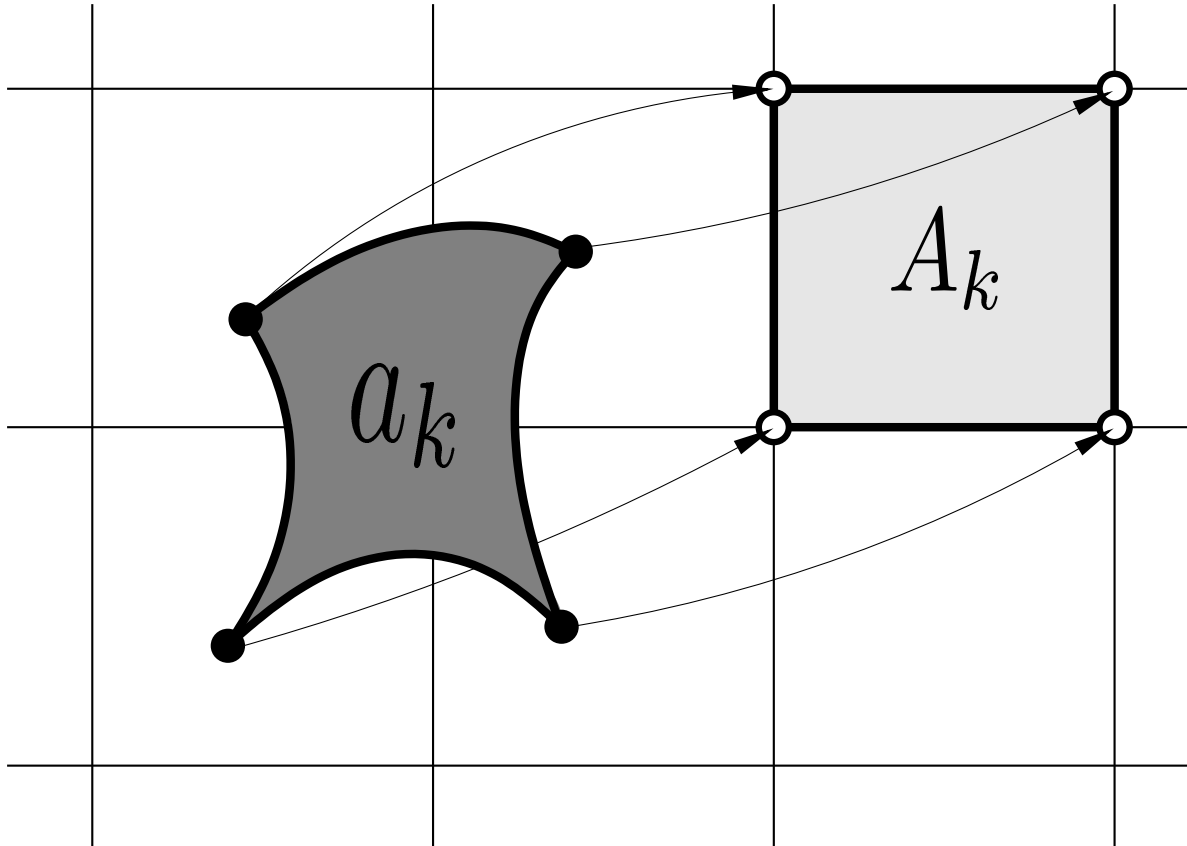
Some things that I will NOT talk about

3. Gone through exercise of smoothing PHIS for spectral-element dynamical core (height smoothing is only “trivial” for spectral transform dynamical cores!)



Some things that I will NOT talk about

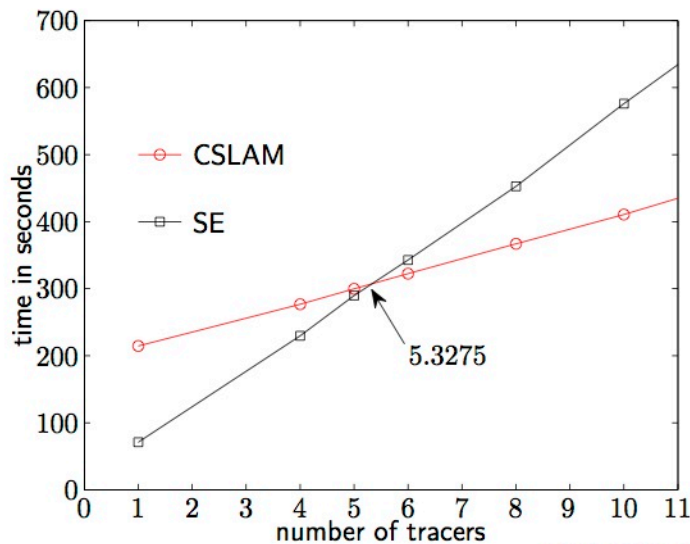
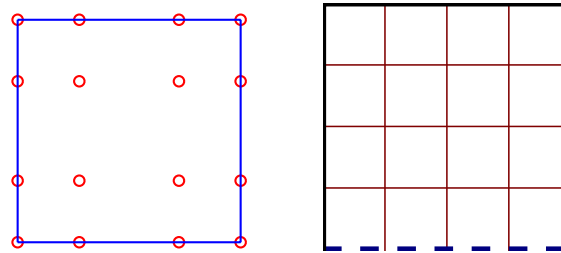
4. CSLAM (Conservative Semi-Lagrangian Multi-tracer scheme) developments:



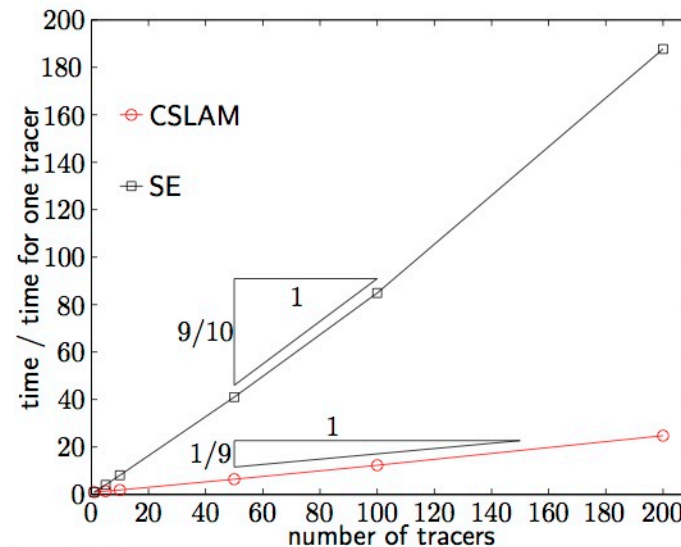
Some things that I will NOT talk about

4. CSLAM (Conservative Semi-Lagrangian Multi-tracer scheme) developments:

a. Implemented in spectral element (SE) dynamical core for inert transport (Erath et. al. 2012)



NCAR's Cray XT5m



Some things that I will NOT talk about

4. CSLAM (Conservative Semi-Lagrangian Multi-tracer scheme) developments:

a. Implemented in spectral element (SE) dynamical core for inert transport (Erath et. al. 2012)

b. CSLAM-SW: shallow water model with semi-implicit CSLAM time-stepping (consistent transport)

Wong, May, William C. Skamarock, Peter H. Lauritzen, Roland B. Stull, 2013: A Cell-Integrated Semi-Lagrangian Semi-Implicit Shallow-Water Model (CSLAM-SW) with Conservative and Consistent Transport. *Mon. Wea. Rev.*, 141, 2545–2560.

c. CSLAM-NH: non-hydrostatic fully compressible semi-implicit solver in x-z plane with consistent tracer transport

PhD thesis : M. Wong (University of British Columbia, Vancouver; UBC)

PhD committee : Skamarock (NCAR), Lauritzen (NCAR), Stull (UBC)



Outline

2. “Toy chemistry” Beyond linear transport scheme tests ...

1. **Results** from a collection of state-of-the-art transport scheme (including ICON) exercising new standard test case suite:

Geosci. Model Dev., 5, 887–901, 2012
www.geosci-model-dev.net/5/887/2012/
doi:10.5194/gmd-5-887-2012
© Author(s) 2012. CC Attribution 3.0 License.



A standard test case suite for two-dimensional linear transport on the sphere

P. H. Lauritzen¹, W. C. Skamarock¹, M. J. Prather², and M. A. Taylor³

Why focus on transport ?

- **Almost** all major modeling centers are developing **new scalable dynamical cores** – a transport operator is a basic building block!
 - **Accurate** tracer transport is becoming increasingly important:
 - Microphysics: mass & number concentrations for water vapor, cloud ice & liquid (rain, snow, ..)
 - Aerosols: sulfate, black carbon, etc. accounted for in three modes
 - Chemical species
 - **large gradients, features “collapse” to the grid scale, ...**
 - Consistent air density and tracer mass transport!
 - **particularly important for chemistry**
 - Tracer transport can account for most of the computational cost of “resolved” scale dynamics computations
 - e.g., 26+ tracers to prognose in CAM5; 126+ in chemistry version
- Multi-tracer efficiency** is becoming increasingly important
- Compute architectures are changing: **“Multi-everything”**



Most widely used test case in the literature (global models) ?

A Standard Test Set for Numerical Approximations to the Shallow Water Equations in Spherical Geometry

DAVID L. WILLIAMSON

The National Center for Atmospheric Research, Boulder, Colorado 80307

JOHN B. DRAKE

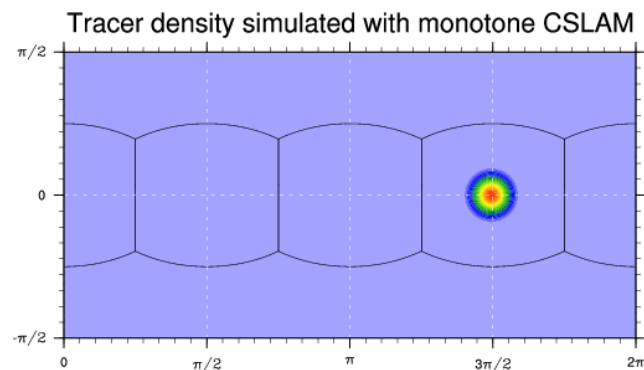
Oak Ridge National Laboratory, Oak Ridge, Tennessee 37831

AND

JAMES J. HACK, RÜDIGER JAKOB, AND PAUL N. SWARZTRAUBER

The National Center for Atmospheric Research, Boulder, Colorado 80307

Received June 17, 1991



Test 1: Solid-body advection

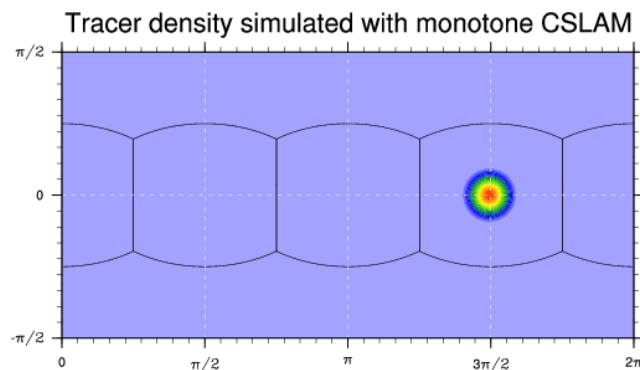
Most widely used test case in the literature (global models) ?

1. No deformation only translation:

-> Flow does not force tracer features to collapse to the grid scale (as they do in real applications)

2. No forcing/physics

Experienced modelers know that schemes that may perform well in idealized settings may “fail” when adding moist physics ...!



Test 1: Solid-body advection

Part 2



THE TERMINATOR TEST



Go a step beyond inert transport testing, that is, add non-linear forcing to idealized flow problem!

At the same time keep things simple enough to be able determine/understand cause and effect

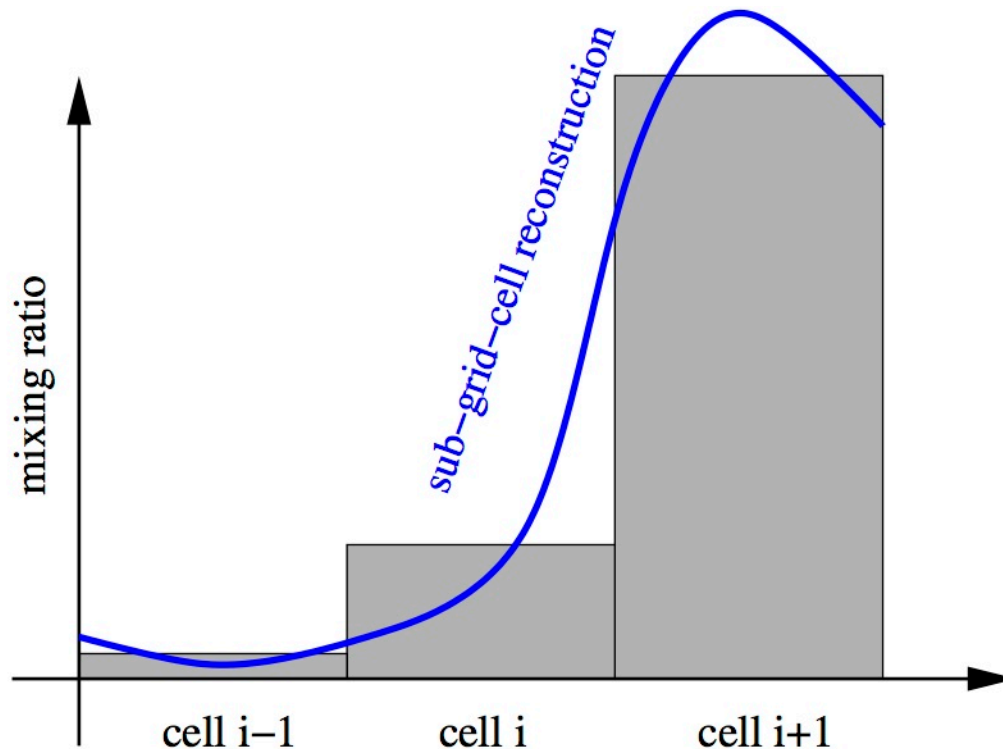
An option: simplified chemical reactions
(right-hand side is products of mixing ratios)



Longer term motivation

Create a simple framework to investigate possible benefits/issues with “higher-order” spatial coupling between dynamics and physics:

- running physics on a different grid than dynamics
- pass sub-grid-scale variance of tracers (from dynamics) to physics



Continuous equations:

$$\frac{D\phi_1}{Dt} = -k_1 \phi_1 \times \phi_2,$$
$$\frac{D\phi_2}{Dt} = -k_2 \phi_1 \times \phi_2.$$

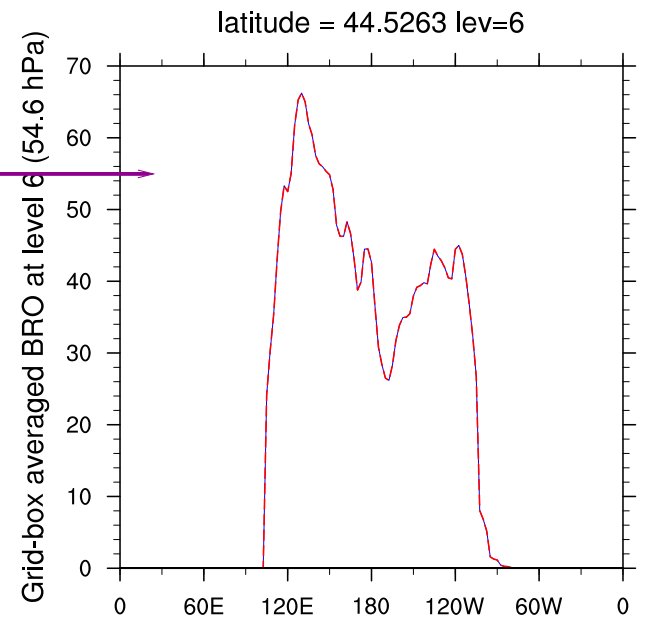
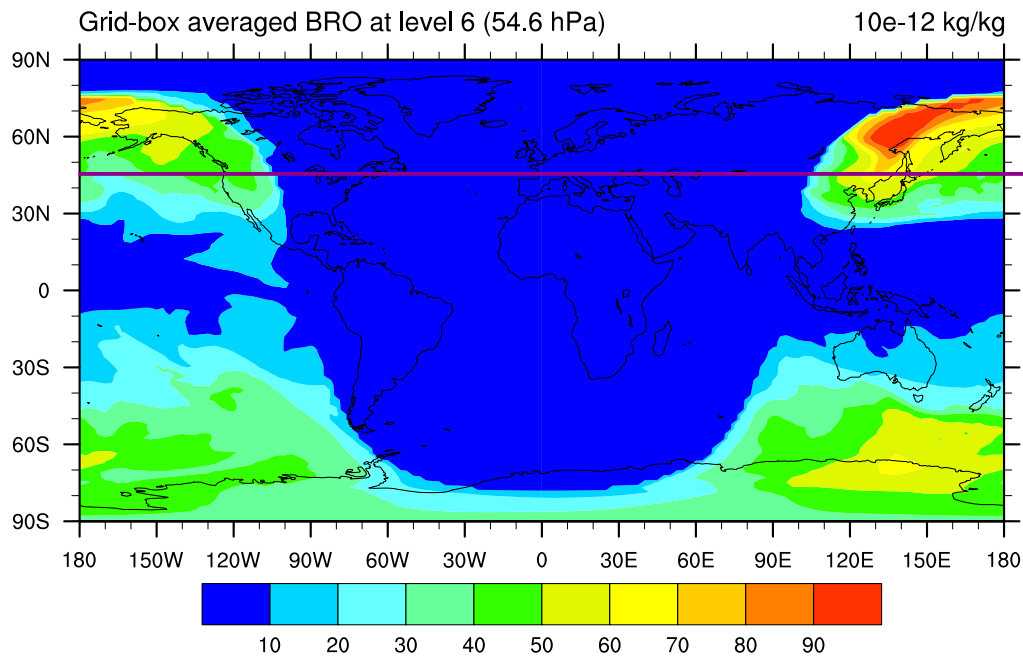
Standard "finite-volume" discretization:

$$\frac{D\bar{\phi}_1}{Dt} = -k_1 \bar{\phi}_1 \times \bar{\phi}_2,$$
$$\frac{D\bar{\phi}_2}{Dt} = -k_2 \bar{\phi}_1 \times \bar{\phi}_2.$$

Include "some" sub-grid-scale variability on right-hand-side:

$$\frac{D\bar{\phi}_1}{Dt} = -k_1 (\bar{\phi}_1 + \phi'_1) \times (\bar{\phi}_2 + \phi'_2),$$
$$\frac{D\bar{\phi}_2}{Dt} = -k_2 (\bar{\phi}_1 + \phi'_1) \times (\bar{\phi}_2 + \phi'_2).$$

“Inspiration” 1: Photolysis driven chemistry



“Inspiration” 2: “Preserving sums”

Chlorine (in CAM-chemistry)

Total Organic Chlorine (set at the surface)

$$T_{Cl}^{ORG} = CH_3Cl + 3CFCl_3 + 2CF_2Cl_2 + 3ClCl_2FCF_2 + HCF_2Cl + 4CCl_4 + 3CH_3CCl_3. \quad (15)$$

Total Inorganic Chlorine (created from break down of T_{Cl}^{ORG})

$$T_{Cl}^{INORG} = Cl + ClO + OClO + 2Cl_2 + 2Cl_2O_2 + HOCl + ClONO_2 + HCl, \quad (16)$$

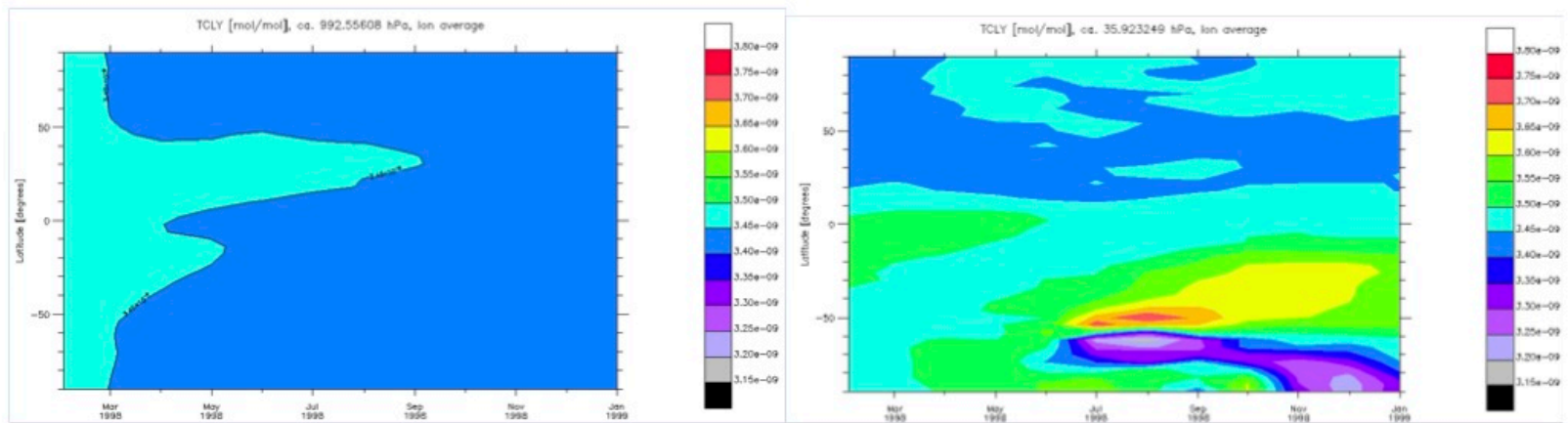
Total Chlorine

$$TCLY = T_{Cl}^{ORG} + T_{Cl}^{INORG} \quad (17)$$

Total chlorine TCLY should be conserved in the upper troposphere and stratosphere (despite complex chemical reactions between the different chlorine species)!

Reactants	Products	Rate
PAN + M	→ CH ₃ CO ₃ + NO ₂ + M	$k(CH_3CO_3+NO_2+M) \cdot 1.11E28 \cdot \exp(-14000/T)$
CH ₃ CO ₃ + CH ₃ CO ₃	→ 2·CH ₃ O ₂ + 2·{CO ₂ }	$2.50E-12 \cdot \exp(500/T)$
GLYALD + OH	→ HO ₂ + 2·GLYOXAL + .8·CH ₂ O + .8·{CO ₂ }	1.00E-11
GLYOXAL + OH	→ HO ₂ + CO + {CO ₂ }	1.10E-11
CH ₃ COOH + OH	→ CH ₃ O ₂ + {CO ₂ } + H ₂ O	7.00E-13
C ₂ H ₅ OH + OH	→ HO ₂ + CH ₃ CHO	$6.90E-12 \cdot \exp(-230/T)$
C ₃ H ₆ + OH + M	→ PO ₂ + M	$k_o=8.00E-27 \cdot (300/T)^{3.50};$ $k_i=3.00E-11; f=0.50$

“Inspiration” 2: “Preserving sums”



(left) longitude-averaged surface TCLY as a function of time and latitude: Constant!
(right) same as (left) but near tropopause: Spurious 7% deviations (near sharp gradients)!

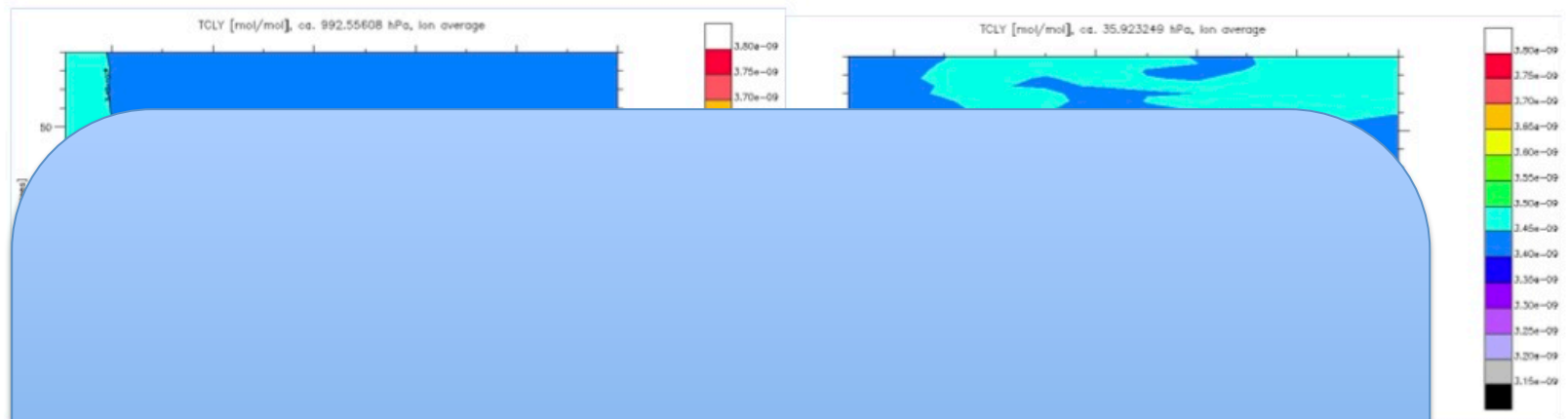
Problem?

Transport scheme can not maintain the sum when transporting the species individually:

$$\sum_{i=1}^{N_X} \mathcal{T}(\chi_i) \neq \mathcal{T} \left(\sum_{i=1}^{N_X} \chi_i \right), \quad (15)$$

where N_X is the number of species χ_i .

“Inspiration” 2: “Preserving sums”



For a test to assess how well sums are preserved for inert linear transport (no chemistry) see Lauritzen and Thuburn (2011, QJRMS)

(left)
(right)

constant!
gradients)!

Prob
Tran

dividually:

(15)

where N_x is the number of species χ_i .

Beyond passive idealized transport testing: “Toy” chemistry

Two Chlorine species (Cl and Cl₂) that react non-linearly: $k_1 \gg k_2$ - terminator
Total amount of Chlorine ($Cly = 2 \cdot Cl + Cl_2$) is conserved.

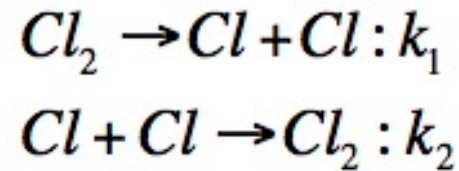
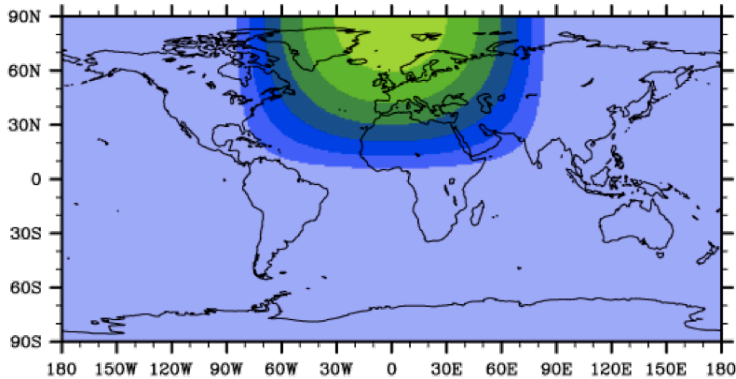


Figure shows k_1 (k_2 is constant)

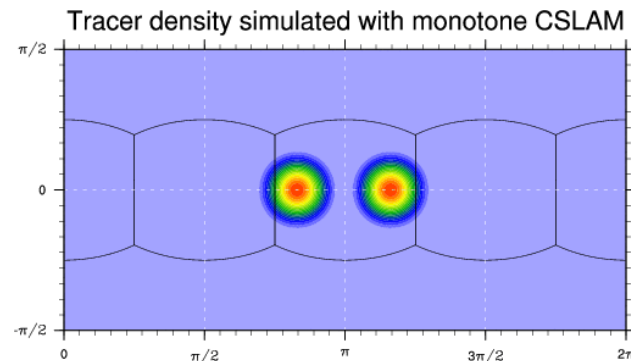
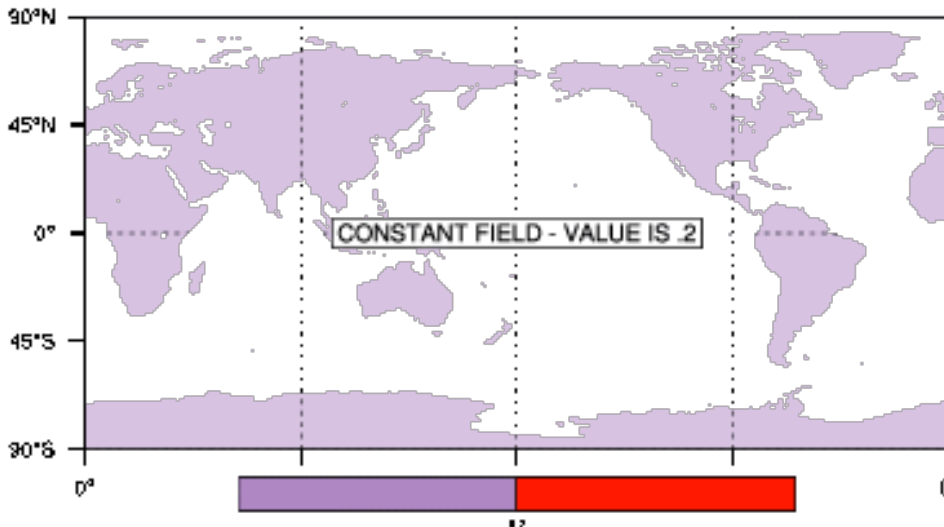
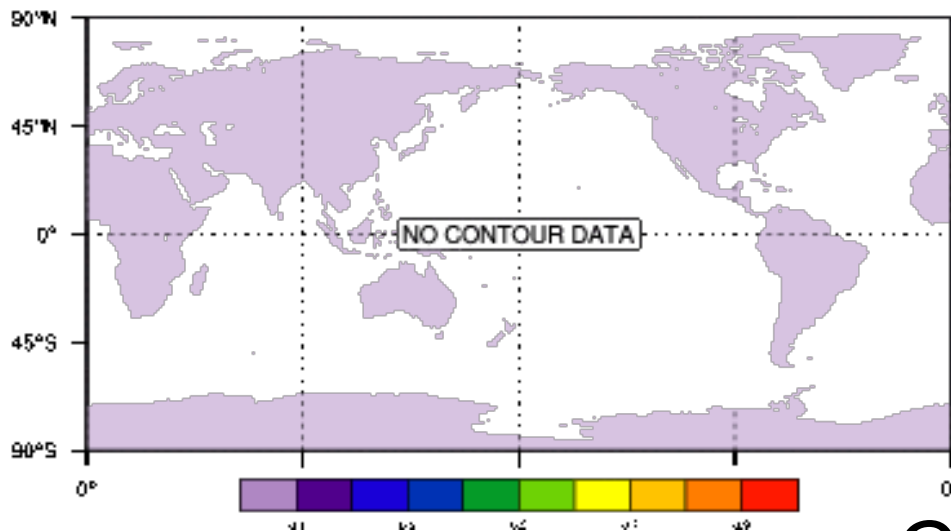
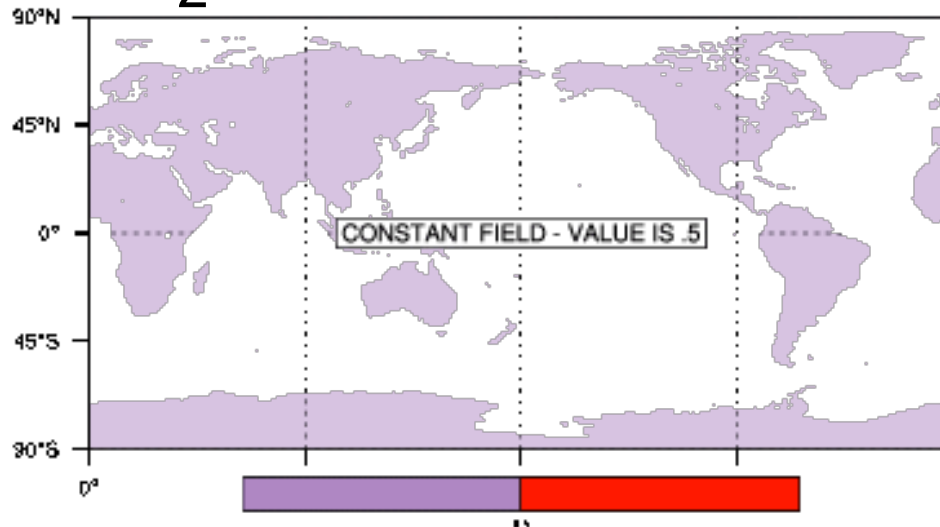


Figure illustrating
Flow field

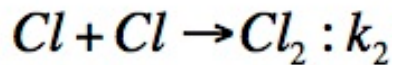
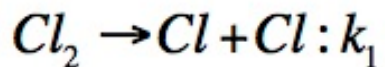
Cl



Cl₂



Non-linear
"terminator-toy"
chemistry:



$$Cl_y = Cl + 2 * Cl_2$$

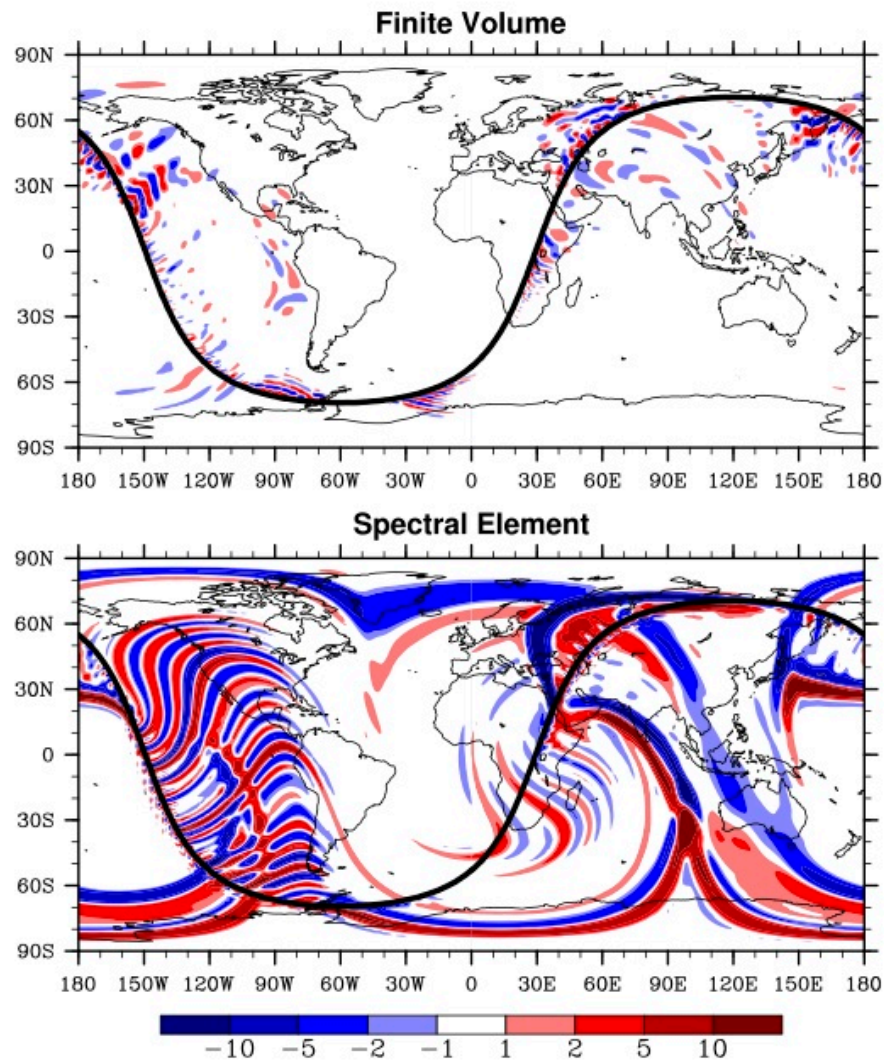


Figure 1. Distribution of the difference (in %) between Cl_y as simulated by the FV (top) and SE (bottom) dynamical cores and the value it would have under a perfectly accurate transport scheme. The thick black line indicates the position of the terminator line defined by the fast reaction rate specified to be similar to a photolysis rate. Results are shown for an instantaneous snapshot after 10 days of simulation.

These are the basic ideas ...

**Exact test case specification is still
work-in-progress ...**



Part 1



Design objectives

Facilitate scheme intercomparison (model development)
(specific guidelines on resolution, test case configuration)

Assess important aspects of accuracy in geophysical fluid dynamics (that we believe current idealized testing does not!) using a “minimal” test case suite

Keep things simple !!!!

Only 2 analytical wind fields and 4 initial conditions – the rest is diagnostics!

(almost any test case suite could be extended to include more tests that could provide more insights into specific aspects of accuracy particularly useful for some classes of schemes and applications)

Assume that scheme developers have already tested their scheme with simpler test cases (solid-body rotation, etc.) and we do not ask modelers to report on them



community asked to bring solutions to new test suite

NCAR Workshop (March, 2011)

Passive & inert idealized 2D transport test cases designed to assess:

1. Numerical order of convergence (C^∞ initial conditions) – Δx in $[0.3^\circ, 3^\circ]$
2. “Minimal” resolution (C^1 initial conditions)
3. Ability of transport scheme to preserve filaments
4. Ability of transport scheme to transport “rough” distributions
5. Ability of the transport scheme to preserve pre-existing functional relations between species (e.g., N_2O - NO_y , family of species, ...)

under challenging flow conditions

$$u(\lambda, \theta, t) = \kappa \sin(2\lambda') \sin(2\theta) \cos(\pi t/T) + 2\pi \cos(\theta)/T$$

$$v(\lambda, \theta, t) = \kappa \sin(2\lambda') \cos(\theta) \cos(\pi t/T),$$

(Nair and Lauritzen, 2010, JCP).

6. Transport under divergent flow conditions (forces modelers to consider coupling between air and tracer mass; at least for finite-volume based schemes)





Geosci. Model Dev., 5, 887–901, 2012
www.geosci-model-dev.net/5/887/2012/
doi:10.5194/gmd-5-887-2012
© Author(s) 2012. CC Attribution 3.0 License.



A standard test case suite for two-dimensional linear transport on the sphere

P. H. Lauritzen¹, W. C. Skamarock¹, M. J. Prather², and M. A. Taylor³

¹National Center for Atmospheric Research, Boulder, Colorado, USA

²Earth System Science Department, University of California, Irvine, California, USA

³Sandia National Laboratories, Albuquerque, New Mexico, USA

<http://www.geosci-model-dev.net/5/887/2012/gmd-5-887-2012.pdf>



Date: 5 July 2013
A standard test case suite for two-dimensional linear transport on the sphere: results from a collection of state-of-the-art schemes

P.H. Lauritzen¹, P.A. Ullrich¹⁴, P. A. Bosler², D. Calhoun³, A.J. Conley¹, T. Enomoto⁴, L. Dong⁵, S. Dubey⁶, O. Guba⁷, A.B. Hansen¹⁰, C. Jablonowski², E. Kaas⁹, J. Kent², J.-F. Lamarque¹, M.J. Prather¹², D. Reinert¹³, V.V. Shashkin¹⁵, W.C. Skamarock¹, B. Sørensen⁹, M.A. Taylor⁷, M.A. Tolstykh¹⁵, and J.B. White III¹

¹National Center for Atmospheric Research, Boulder, Colorado, USA^a

²University of Michigan, Department of Atmospheric, Oceanic and Space Sciences, Ann Arbor, Michigan, USA

³Boise State University, Boise, Idaho, USA

⁴Disaster Prevention Research Institute, Kyoto University, Uji, Kyoto, Japan

⁵State Key Laboratory of Numerical Modeling for Atmospheric Sciences and Geophysical Fluid Dynamics, Institute of Atmospheric Physics, Chinese Academy of Sciences, Beijing, People's Republic of China

⁶Laboratoire de Météorologie Dynamique, Paris, France

⁷Sandia National Laboratories, Albuquerque, New Mexico, USA

⁸Environmental Modeling Center, National Centers for Environmental Prediction, Maryland, USA

⁹Niels Bohr Institute, University of Copenhagen, Copenhagen, Denmark

¹⁰Department of Environmental Science, Aarhus University, Aarhus, Denmark

¹¹Forschungszentrum Jülich, Germany

¹²Earth System Science Department, University of California, Irvine, California, USA

¹³Deutscher Wetterdienst, Offenbach, Germany

¹⁴University of California at Davis, Davis, California, USA

¹⁵Hydrometcentre of Russia, Moscow, Russia

Lauritzen et al., 2013, "almost done")



Comparison/"database" manuscript:

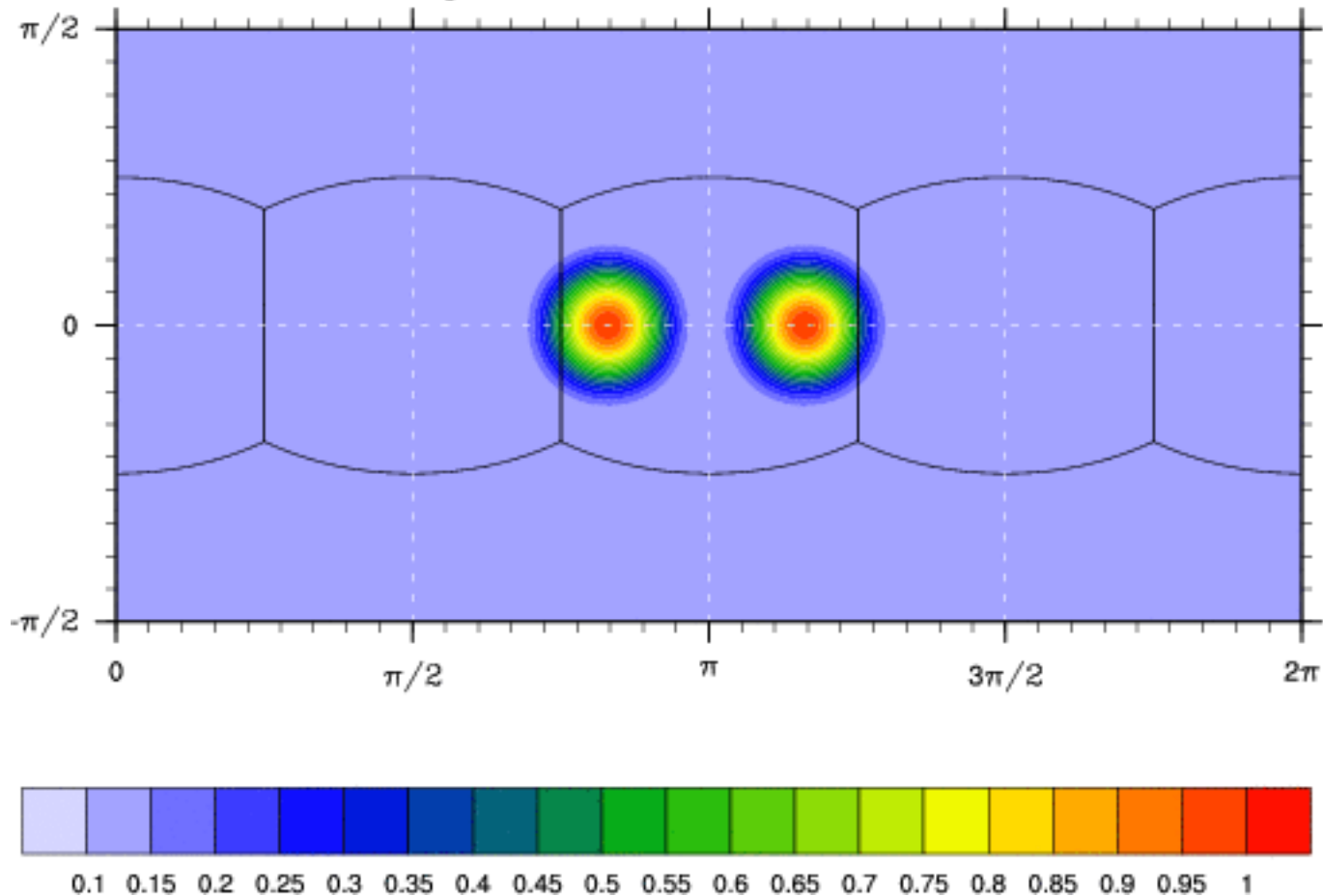
Table 1. A list of acronyms (first column), full names (second column), documentation (third column), implementation grid (fourth column), and formal order of accuracy (fifth column) for schemes in this paper.

scheme acronym	full scheme name	documentation	implementation grid	formal order
CAM-FV	Community Atmosphere Model - Finite-Volume	Lin and Rood (1996) Lin (2004)	Regular latitude-longitude	2
CAM-SE	Community Atmosphere Model - Spectral Elements	Dennis et al. (2012) Neale et al. (2010); Guba et al. (2013)	Gnomonic cubed-sphere (quadrature grid)	4
CCSRG	Conservative cascade scheme for the reduced grid	Nair et al. (2002) Tolstykh and Shashkin (2012)	Reduced latitude-longitude	3
CLAW	Wave propagation algorithm on mapped grids	LeVeque (2002)	two-patch sphere grid	2
CSLAM	Conservative Semi-Lagrangian Multi-tracer scheme	Lauritzen et al. (2010) Erath et al. (2013)	Gnomonic cubed-sphere	3
FARSIGHT	Departure-point interpolation scheme with a global mass fixer	White and Dongarra (2011)	Gnomonic cubed-sphere	2
HEL	Hybrid Eulerian Lagrangian	Kaas et al. (2013)	Gnomonic cubed-sphere	3
HEL-ND	HEL - Non-Diffusive	Kaas et al. (2013)	Gnomonic cubed-sphere	3
HOMME	High-Order Methods Modeling Environment	Dennis et al. (2012) Guba et al. (2013)	Gnomonic cubed-sphere (quadrature grid)	4 & 7
ICON-FFSL	ICOsahedral Non-hydrostatic model - Flux-Form semi-Lagrangian scheme	Miura (2007)	Icosahedral-triangular	2
LPM	Lagrangian Particle Method	Bosler (2013)	Icosahedral-triangular	2
MPAS	Model for Prediction Across Scales	Skamarock and Gassmann (2011)	Icosahedral-hexagonal	3
SBC	Spectral Bicubic interpolation scheme	Enomoto (2008)	Gaussian latitude-longitude	2
SFF-CSLAM	Simplified Flux-Form CSLAM scheme	Ullrich et al. (2013)	Gnomonic cubed-sphere	3&4
SLFV-SL	Semi-Lagrangian type Slope Limited	Miura (2007)	Icosahedral hexagonal	2
SLFV-ML	Slope Limited Finite Volume scheme with method of lines	Dubey et al. (2012)	Icosahedral hexagonal grid	2
TTS	Trajectory-Tracking Scheme	Dong and Wang (2013)	Spherical centroidal Voronoi tessellation	1
UCISOM	UC Irvine Second-Order Moments scheme	Prather (1986)	Regular latitude-longitude	2
UCISOM-CS	UC Irvine Second-Order Moments scheme	-	Gnomonic cubed-sphere	2

Lauritzen et al., 2013, "almost done")



Tracer density simulated with monotone CSLAM

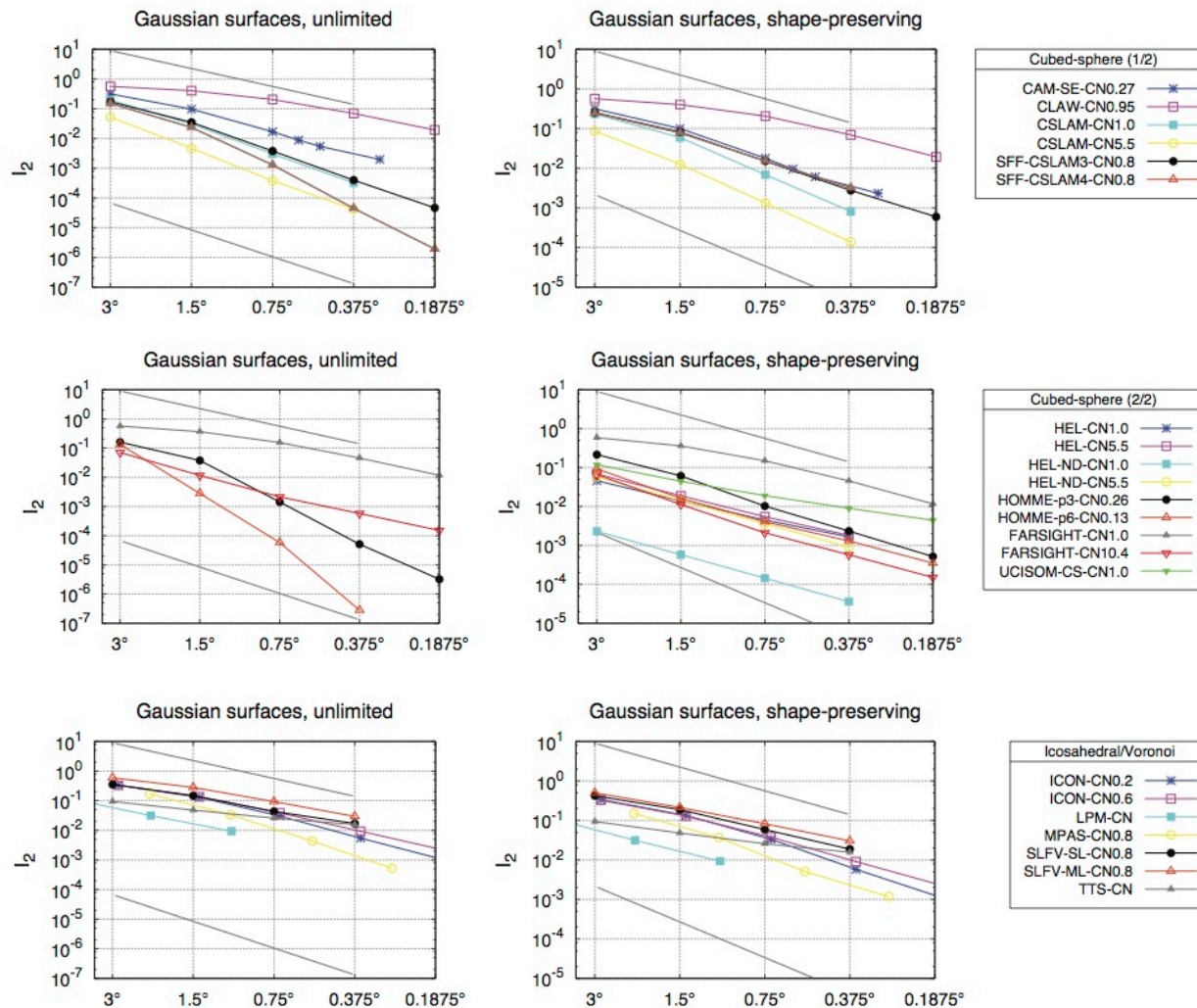


CSLAM = Conservative Semi-Lagrangian Multi-tracer scheme

Lauritzen et al. (2010,JCP), Harris et al. (2011), Lauritzen et al. (2011,JCP)

1. Numerical convergence rate

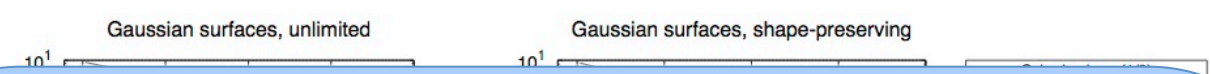
in the resolution range approximately 3° to 0.3° (i.e. from paleo to high resolution climate modeling)



Lauritzen et al. (2013, "almost done"),

1. Numerical convergence rate

in the resolution range approximately 3° to 0.3° (i.e. from paleo to high resolution climate modeling)

- 
- Initial condition and flow (except the poles) is infinitely smooth: Hence schemes should (at high enough resolution) converge at their formal order of accuracy!
 - Slope: Schemes differ significantly in when asymptotic convergence is achieved
 - Absolute values: test diagnostic 2

Lauritzen et al. (2013, “almost done”),



1. Numerical convergence rate

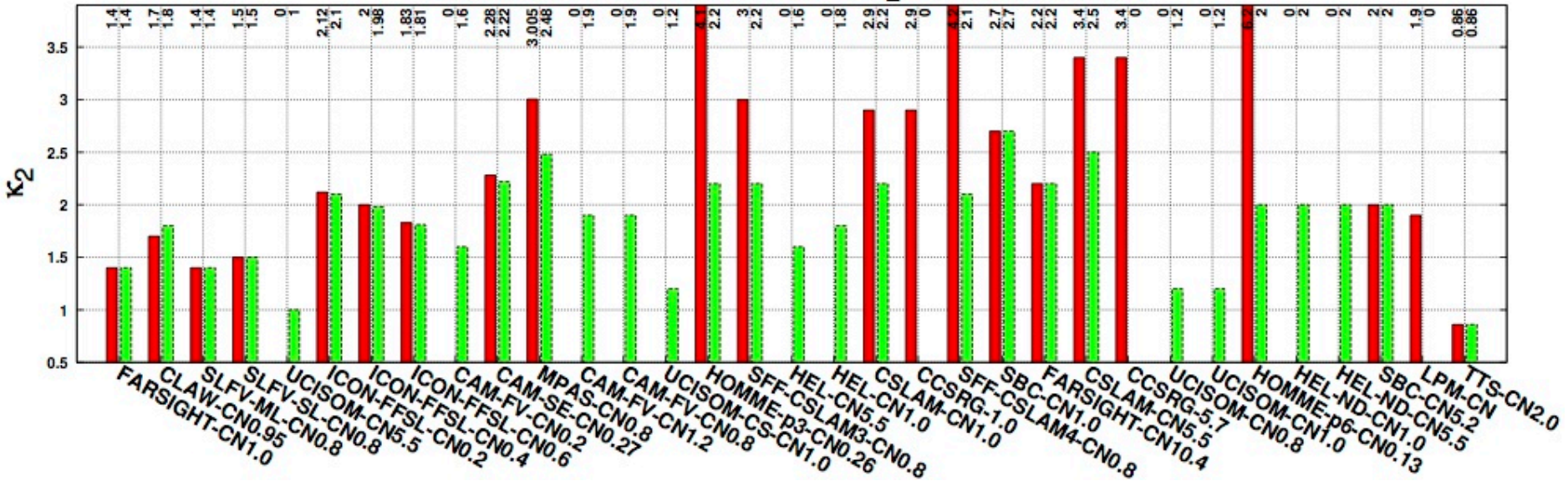
in the resolution range approximately 3° to 0.3° (i.e. from paleo to high resolution climate modeling)

un = unlimited scheme sp = shape-preserving version of scheme

In scheme acronym labels: CN = Courant Number

un █ sp █

optimal convergence rate for l_2 (Gaussian hills)



K_2 = Least-squares regression to l_2 in range $[0.2^\circ, 3^\circ]$

Note: resolution range was deliberately chosen to challenge schemes (for a resolution range with finer resolutions features would be well-resolved)

Lauritzen et al. (2013, "almost done"),

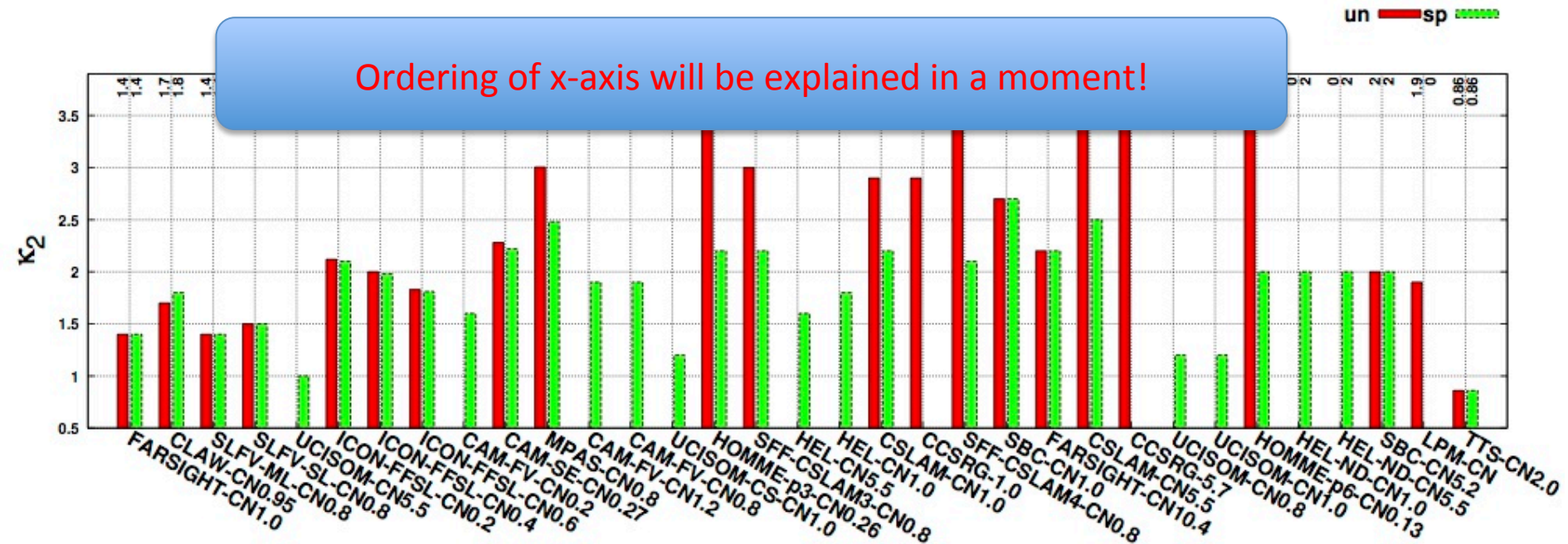
1. Numerical convergence rate

in the resolution range approximately 3° to 0.3° (i.e. from paleo to high resolution climate modeling)

un = unlimited scheme sp = shape-preserving version of scheme

In scheme acronym labels: CN = Courant Number

Ordering of x-axis will be explained in a moment!



K_2 = Least-squares regression to $|2$ in range $[0.2^\circ, 3^\circ]$

Note: resolution range was deliberately chosen to challenge schemes (for a resolution range with finer resolutions features would be well-resolved)

Lauritzen et al. (2013, "almost done"),

1. Numerical convergence rate

in the resolution range approximately 3° to 0.3° (i.e. from paleo to high resolution climate modeling)

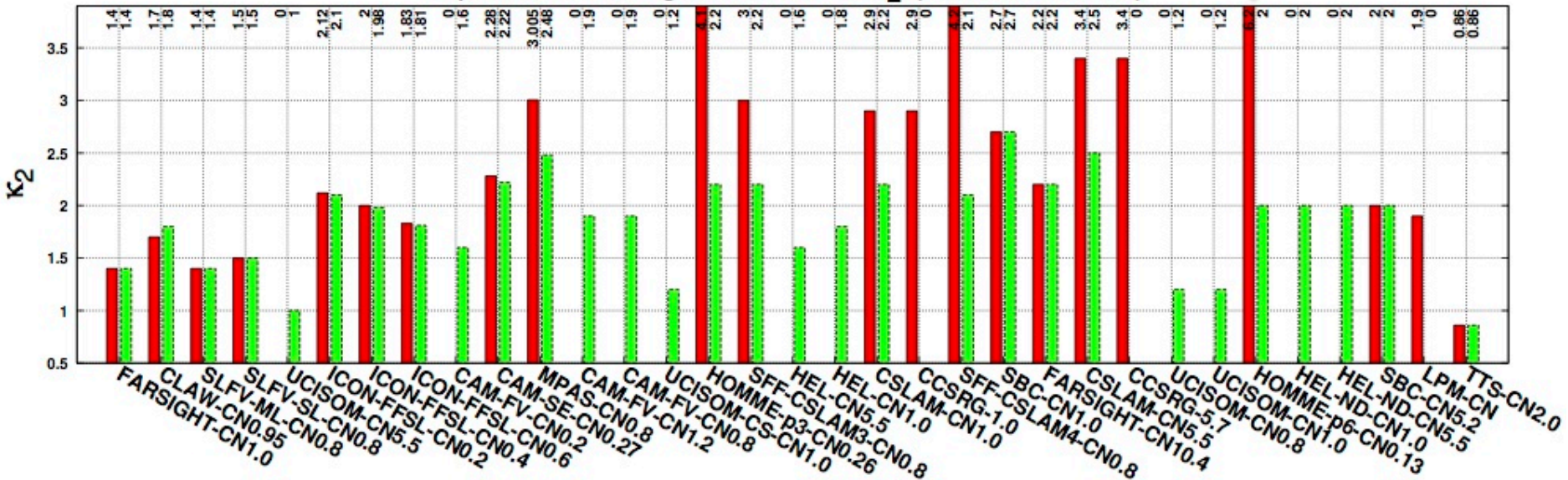
un = unlimited scheme

sp = shape-preserving version of scheme

CN = Courant Number

optimal convergence rate for l_2 (Gaussian hills)

un █ sp █



- Not surprisingly shape-preserving filters/limiters reduce order of convergence
- Some shape-preserving filters/limiters are more “invasive” than others
- For some schemes convergence rates are affected by time-step

Lauritzen et al. (2013, “almost done”),

2. “Minimal” resolution

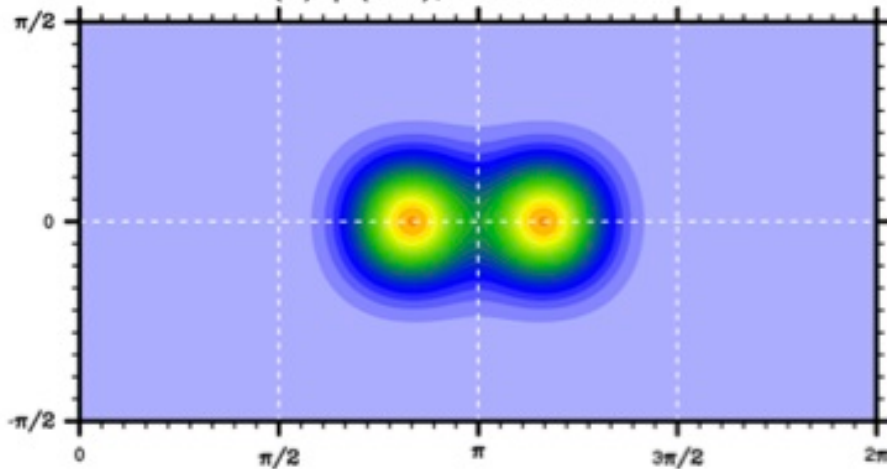
(absolute error)

At what resolution is a certain level of accuracy reached?

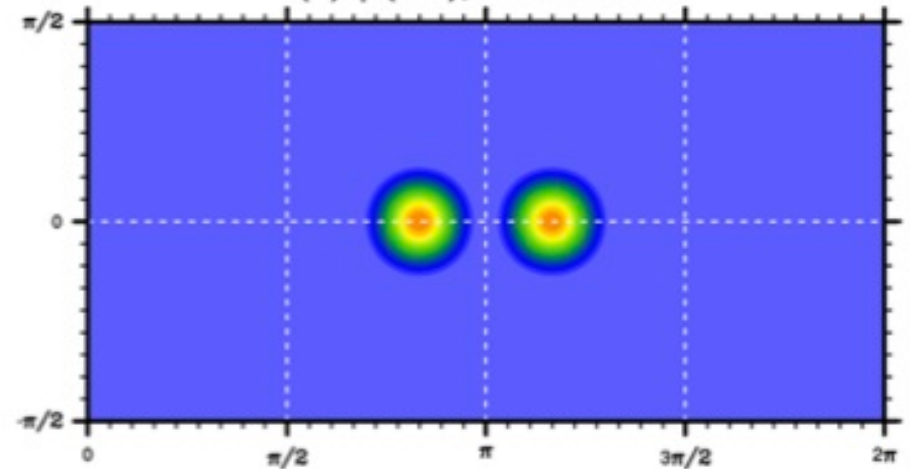
Level of accuracy is defined in terms of RMS type error norm

Now initial conditions are C^1 continuous

(a) $\phi(t=0)$, Gaussian hills



(b) $\phi(t=0)$, cosine bells



Lauritzen et al. (2013, “almost done”),



2. “Minimal” resolution

(absolute error)

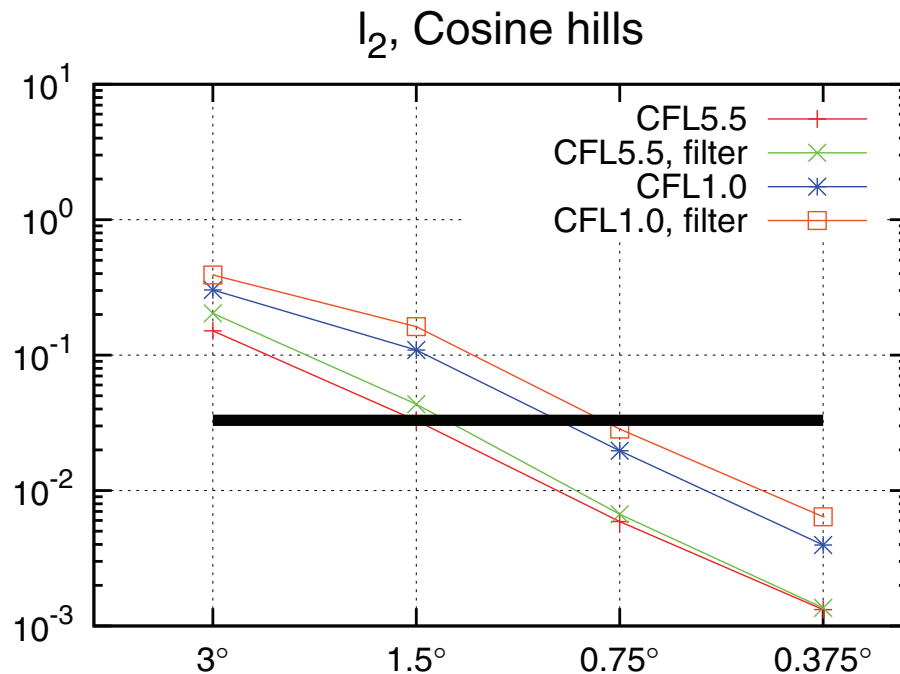


Fig. 5. Convergence plot for l_2 computed with CSLAM with cosine bells initial conditions. The keys are as in Fig. 4. The heavy line is $l_2 = 0.033$ and is used to define “minimal” resolution.

Somewhat subjective choice: the threshold error norm is based on CSLAM

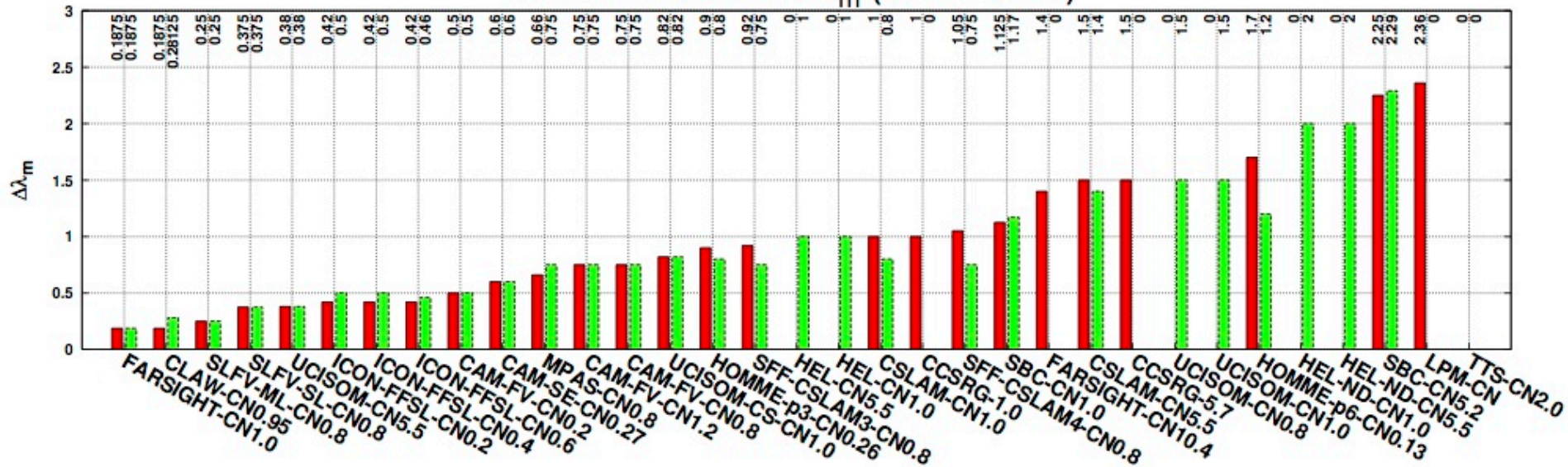
l_2 -error norm for which CSLAM starts to converge asymptotically
(filaments are in some sense resolved!)

Lauritzen et al. (2012, GMD)

2. “Minimal” resolution

(absolute error)

minimal resolution $\Delta\lambda_m$ (Cosine bells)



Minimal resolution varies from 0.2° to 2.3°!

Lauritzen et al. (2013, “almost done”),

“Minimal” resolution and optimal convergence rates

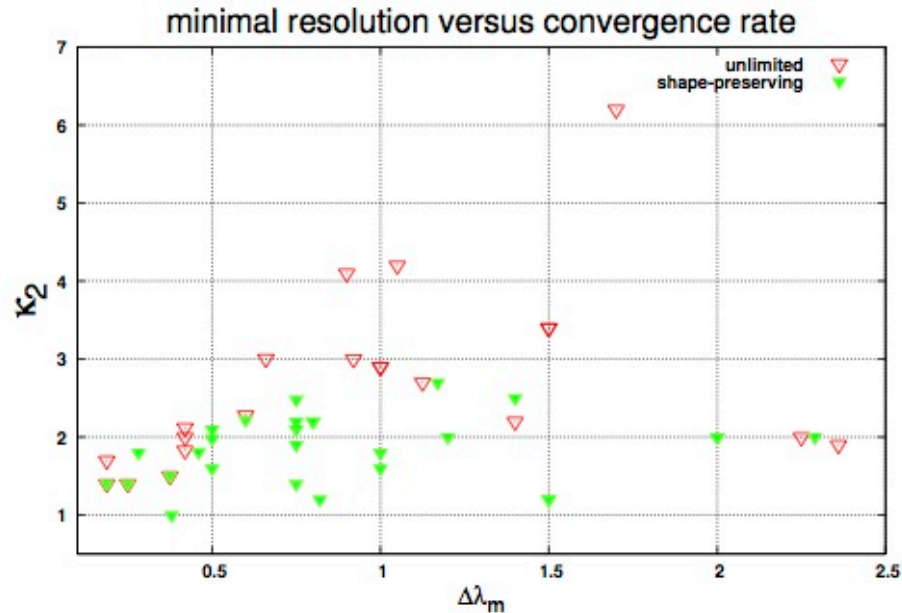
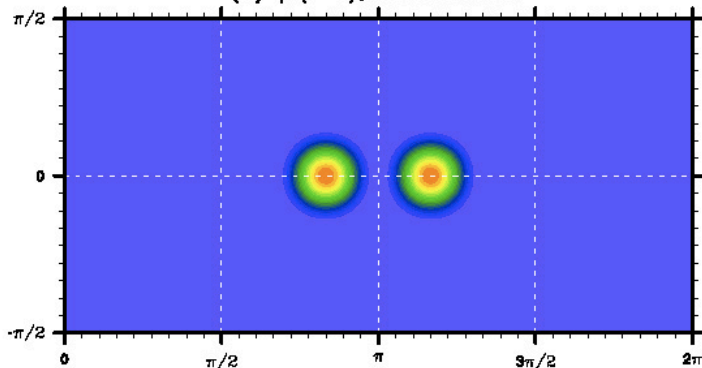


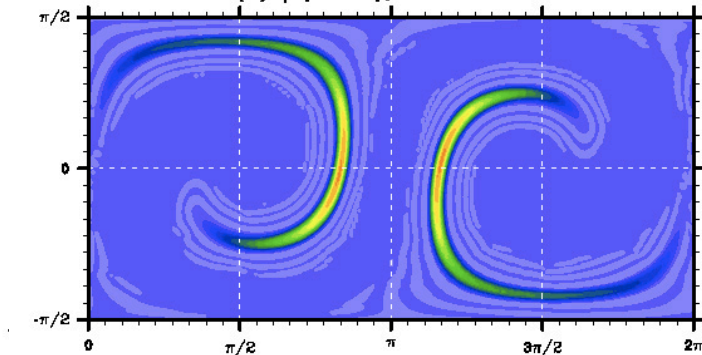
Fig. 4. ‘Scatter-like’ plot of the data shown as histograms on Figure 3 upper and middle rows. Each scheme is represented by a point on the plot with (x,y) coordinates $(\Delta\lambda_m, \kappa_2)$. For clarity each point is not labeled with scheme acronym. The purpose of this Figure is to show that there is not necessary a correlation between ‘optimal’ convergence rate and ‘minimal’ resolution.

3. Filament diagnostic (Prather)

(b) $\phi(t=0)$, cosine bells



(b) $\phi(t=T/2)$, cosine bells



The “filament” preservation diagnostic is formulated as follows. Define $A(\tau, t)$ as the spherical area for which the spatial distribution of the tracer $\phi(\lambda, \theta)$ satisfies

$$\phi(\lambda, \theta) \geq \tau, \quad (27)$$

at time t , where τ is the threshold value. For a non-divergent flow field and a passive and inert tracer ϕ , the area $A(\tau, t)$ is invariant in time.

The discrete definition of $A(\tau, t)$ is

$$A(\tau, t) = \sum_{k \in \mathcal{G}} \Delta A_k, \quad (28)$$

where ΔA_k is the spherical area for which ϕ_k is representative, K is the number of grid cells, and \mathcal{G} is the set of indices

$$\mathcal{G} = \{k \in (1, \dots, K) | \phi_k \geq \tau\}. \quad (29)$$

For Eulerian finite-volume schemes ΔA_k is the area of the k -th control volume. For Eulerian grid-point schemes a control volume for which the grid-point value is representative must be defined. Similarly for fully Lagrangian schemes based on point values (parcels) control volumes for which the point values are representative must be defined. Note that the “control volumes” should span the entire domain without overlaps or “cracks” between them.

Define the filament preservation diagnostic

$$\ell_f(\tau, t) = \begin{cases} 100.0 \times \frac{A(\tau, t)}{A(\tau, t=0)} & \text{if } A(\tau, t=0) \neq 0, \\ 0.0, & \text{otherwise.} \end{cases} \quad (30)$$

For infinite resolution (continuous case) and a non-divergent flow, $\ell_f(\tau, t)$ is invariant in time: $\ell_f(\tau, t=0) = \ell_f(\tau, t) = 100$ for all τ . At finite resolution, however, the filament

This diagnostic does not rely on an analytical solution!

Lauritzen et al. (2013, “almost done”),

3. Filament diagnostic

Diffusive schemes will tend to decrease l_f for higher values of tau and increase l_f for low values of tau:

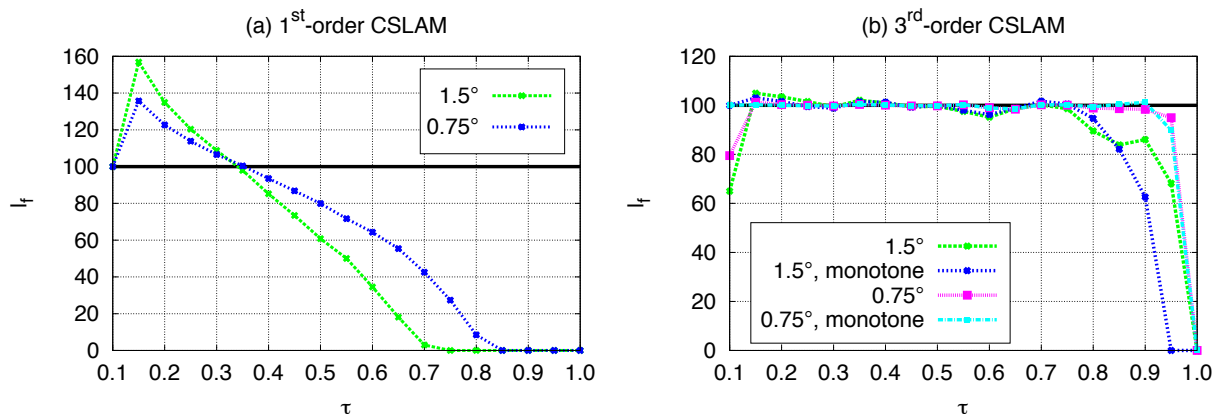
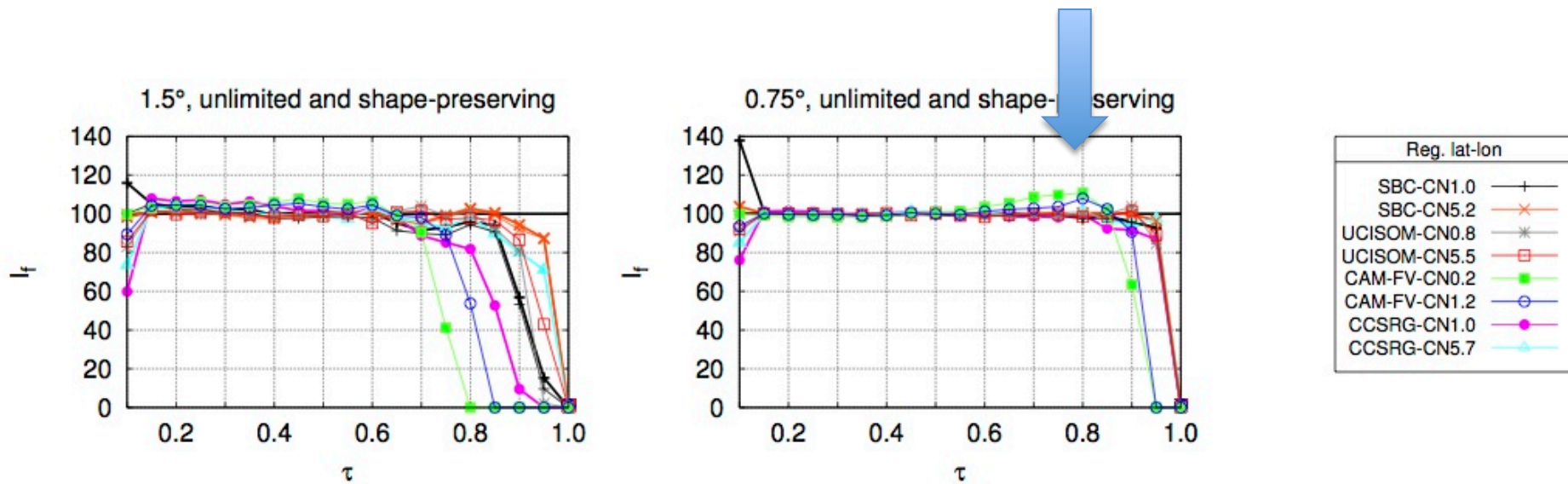


Fig. 6. Filament diagnostics $l_f(t = T/2)$ as a function of threshold value τ for different configurations of the CSLAM scheme with Courant number 5.5. (a) 1st-order version of CSLAM at $\Delta\lambda = 1.5^\circ$ and $\Delta\lambda = 0.75^\circ$, and (b) 3rd-order version of CSLAM with and without monotone/shape-preserving filter at resolutions $\Delta\lambda = 1.5^\circ$ and $\Delta\lambda = 0.75^\circ$.

3. Filament diagnostic

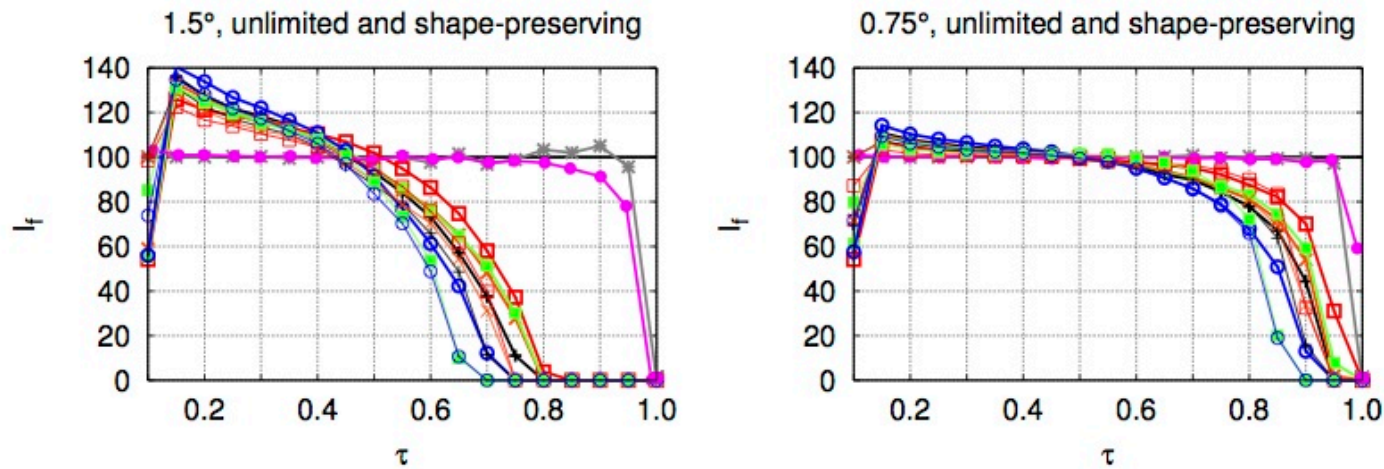
Schemes that steepen gradients will have $I_f > 100$ for higher tau values:



Lauritzen et al. (2013, "almost done"),

3. Filament diagnostic

How is ICON doing?

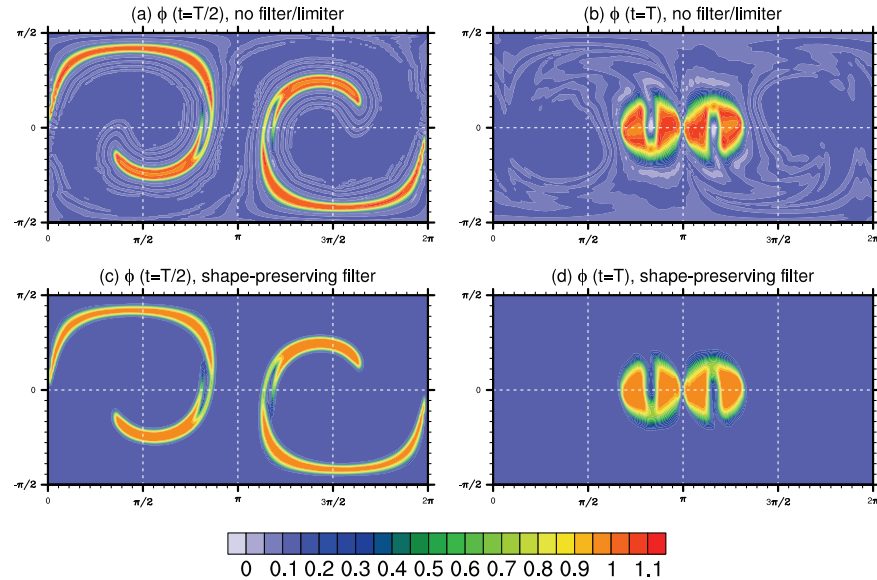
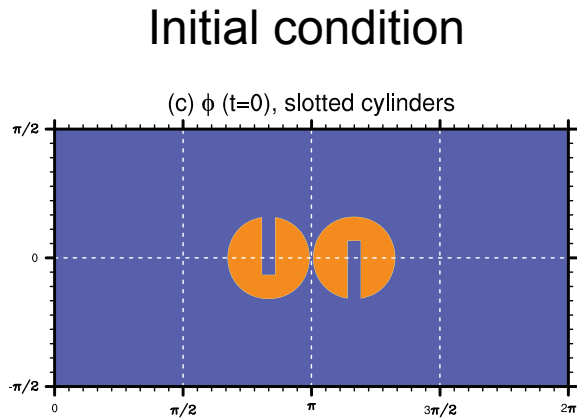


I_f is a smooth and monotone curve 😊

Lauritzen et al. (2013, “almost done”),

4. “Rough” distribution

(to challenge limiters/filters)



Background value is non-zero so positivity preserving filters do not alleviate undershoots!

Fig. 7. Contour plot of the CSLAM numerical solution ϕ at resolution $\Delta\lambda = 1.5^\circ$ and time-step $T/120$ using the slotted-cylinders initial condition at time $t = T/2$ (**a** and **c**) and $t = T$ (**b** and **d**) using no filter/limiter (**a** and **b**) and a shape-preserving filter (**c** and **d**). The standard error norms for the unfiltered/unlimited solution are $\ell_2 = 0.24$, $\ell_\infty = 0.79$, $\phi_{\min} = -0.19$, and $\phi_{\max} = 0.15$, and for the shape-preserving solution they are $\ell_2 = 0.26$, $\ell_\infty = 0.80$, $\phi_{\min} = 0.0$, and $\phi_{\max} = -4.34 \cdot 10^{-3}$.

4. “Rough” distribution

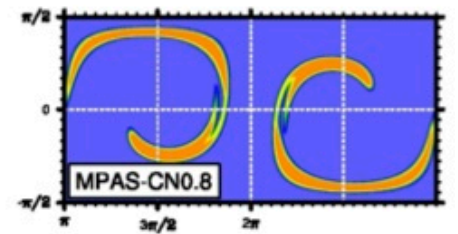
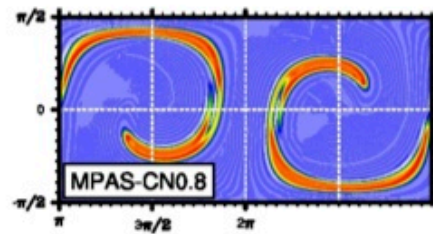
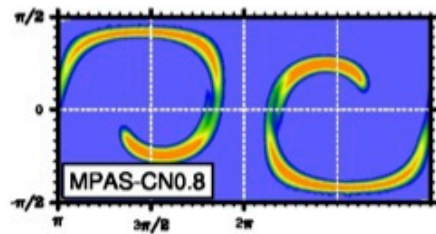
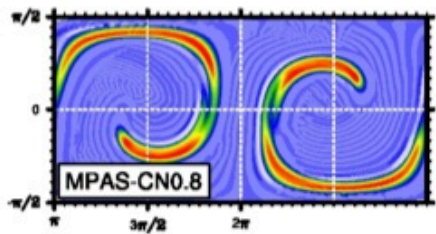
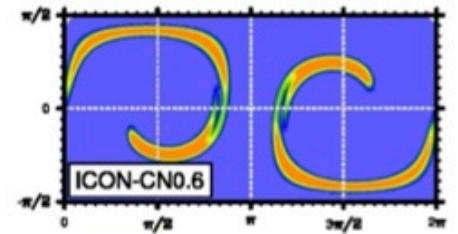
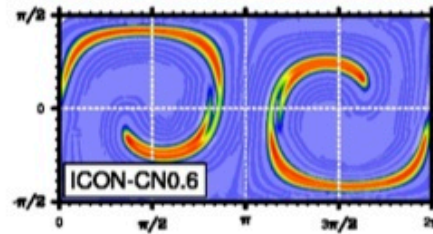
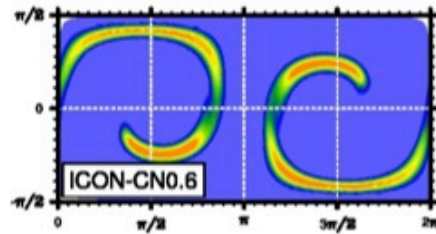
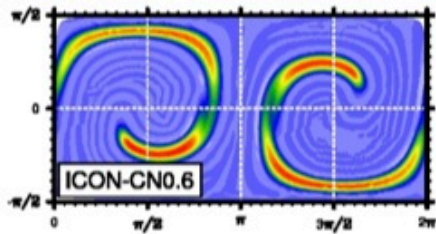
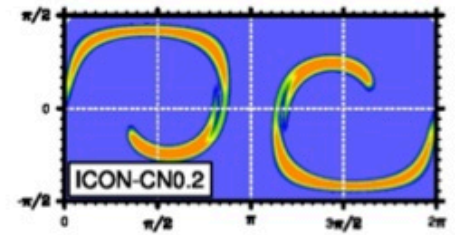
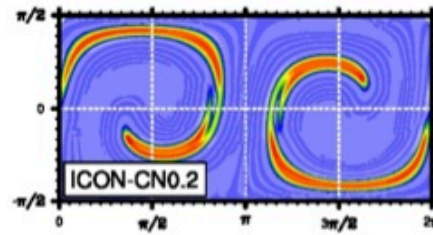
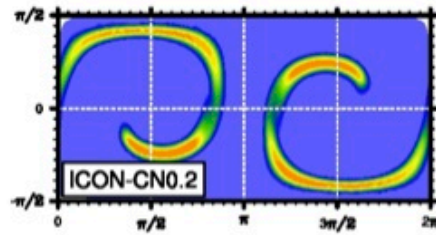
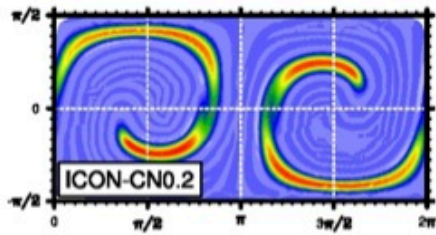
(to challenge limiters/filters)

1.5°, unlimited

1.5°, shape-preserving

0.75°, unlimited

0.75°, shape-preserving



Lauritzen et al. (2013, “almost done”),

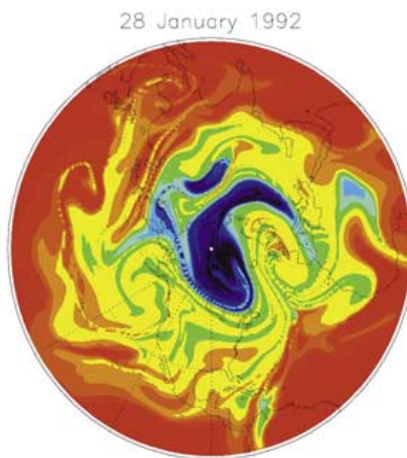
5. Preserving correlations

(the design of schemes that preserve linear correlations was discussed by Lin and Rood (1996) and Thuburn and McIntyre (1997))

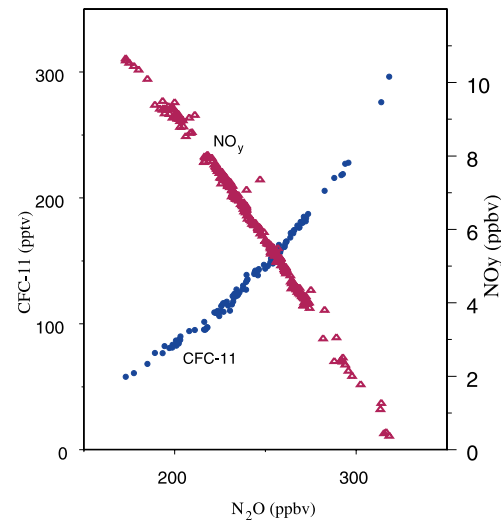
Motivation: Correlations between long-lived species in the stratosphere

Relationships between long-lived stratospheric tracers, manifested in similar spatial structures on scales ranging from a few to several thousand kilometers, are displayed most strikingly if the mixing ratio of one is plotted against another, when the data collapse onto remarkably compact curves. - Plumb (2007)

E.g., when plotting nitrous oxide (N_2O) against 'total odd nitrogen' (NO_y) or chlorofluorocarbon (CFC's)



'inverse filling'



observations

5. Preserving correlations

Motivation: Correlations between long-lived species in the stratosphere

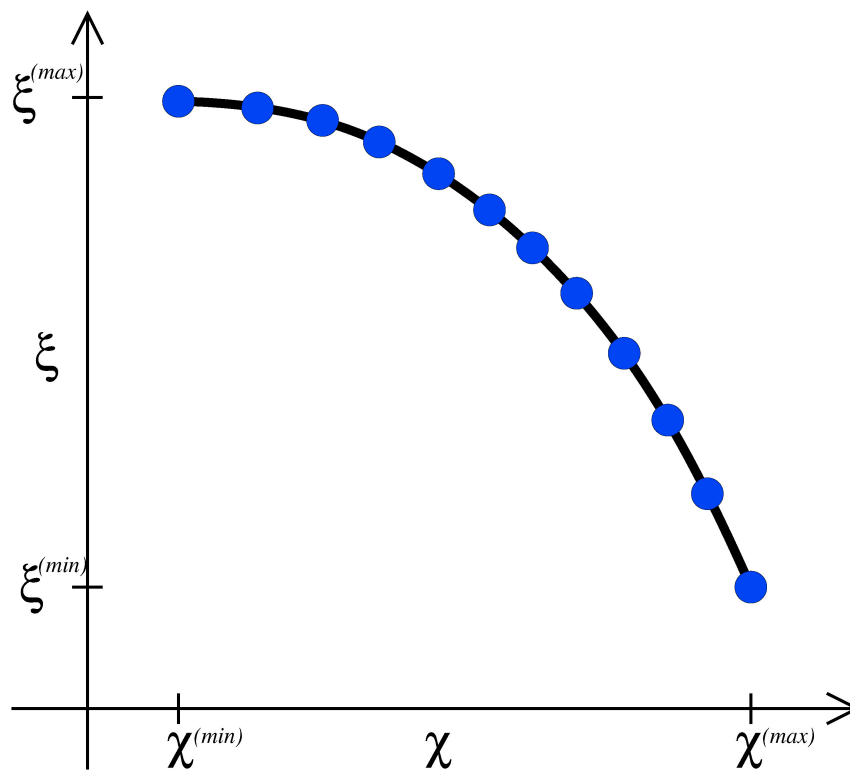
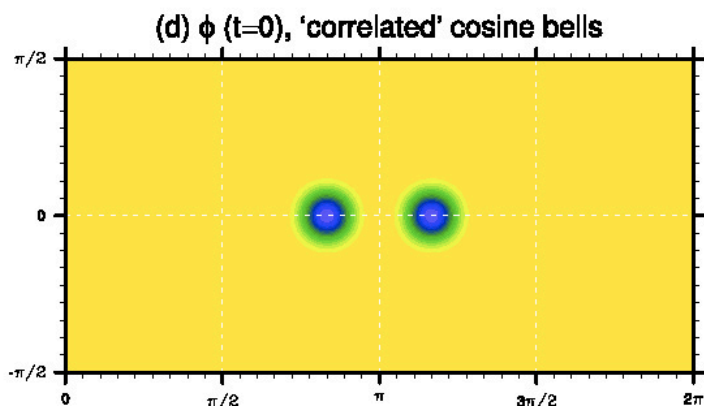
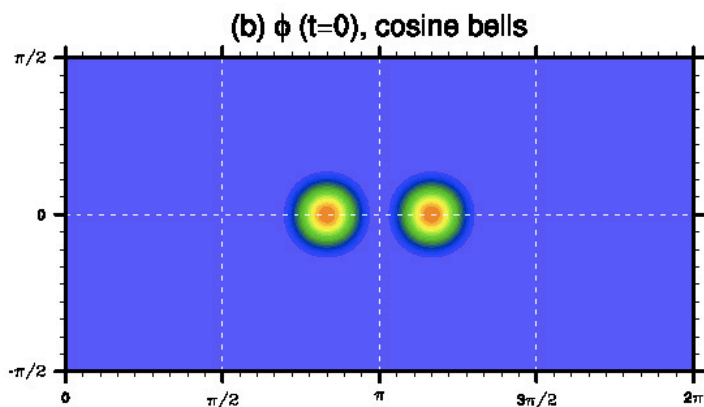
- Such compact scatter plots can be physically or chemically significant; for example, departures from compactness have been used to quantify chemical ozone loss in the ozone hole (Proffitt et al., 1990).
 - → It is therefore highly desirable that transport schemes used in modeling the atmosphere should respect such functional relations and not disrupt them in physically unrealistic ways.
-
- Similarly, the total of chemical species within some chemical family may be preserved following an air parcel although the individual species have a complicated relation to each other and may be transformed into each other through chemical reactions.
 - Similar arguments can be made for aerosol-cloud interactions (Ovtchinnikov and Easter, 2009) where important physical properties are derived from several tracers.

Goal: design idealized test case suite to address some of these aspects of accuracy!

5. Preserving correlations

Initial conditions

tracer 1: cosine bells tracer 2: correlated cosine bells $\Psi(\chi) = a\chi^2 + b$

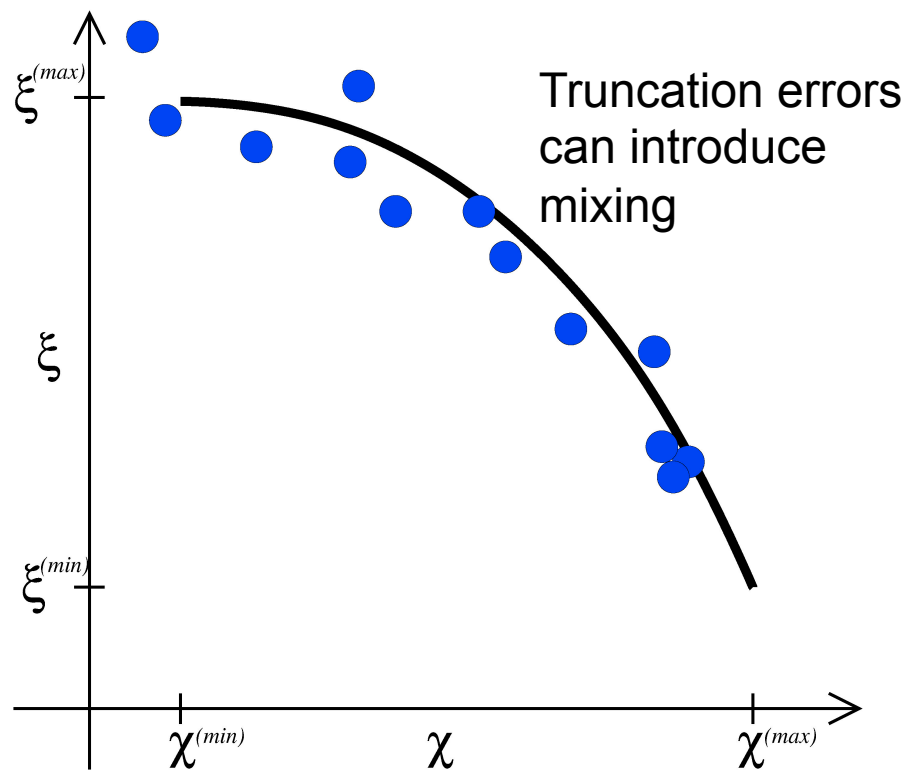
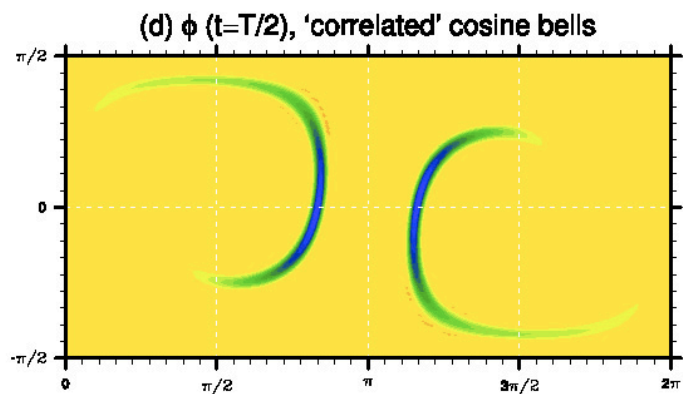
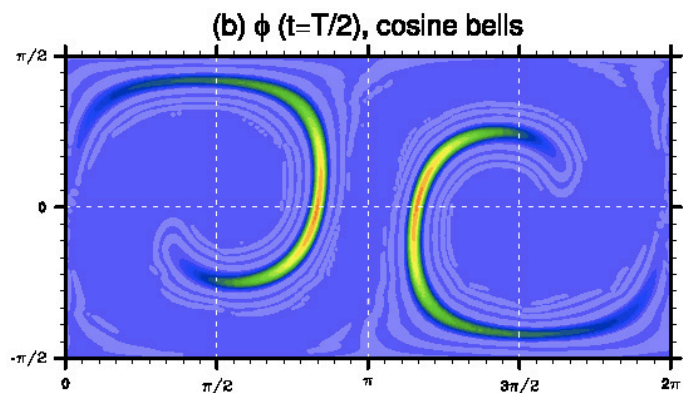


Lauritzen and Thuburn (2011, QJRMS)

5. Preserving correlations

Initial conditions

tracer 1: cosine bells tracer 2: correlated cosine bells $\Psi(\chi) = a\chi^2 + b$

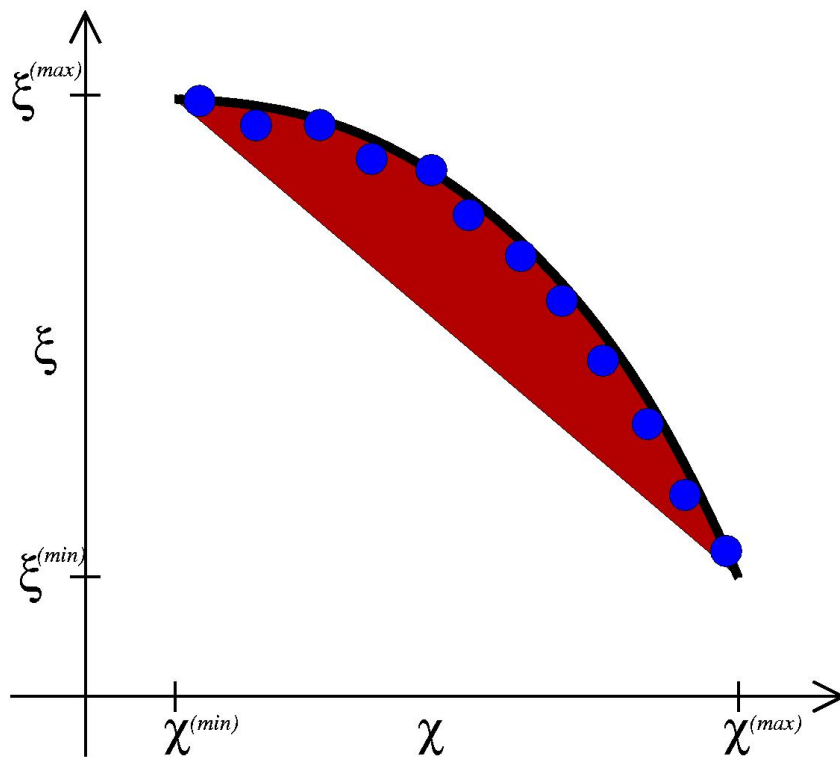


Lauritzen and Thuburn (2011, QJRMS)

5. Preserving correlations

Classification of mixing on scatter plot:

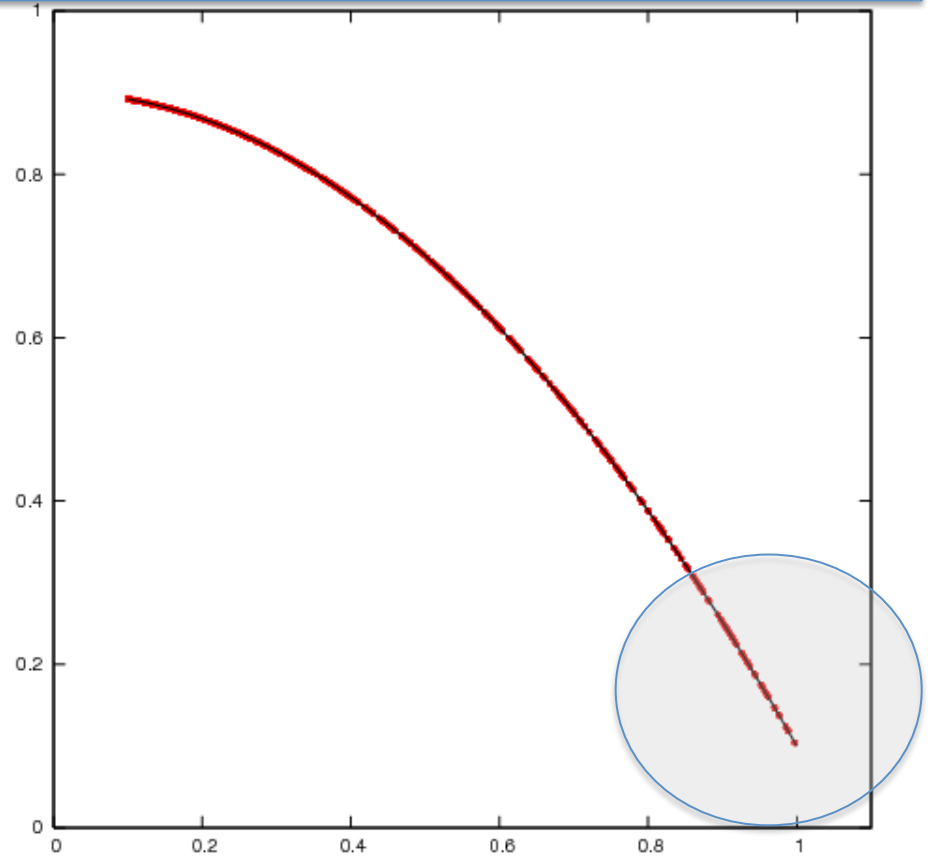
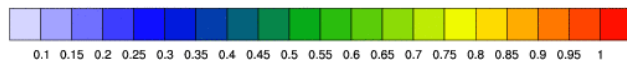
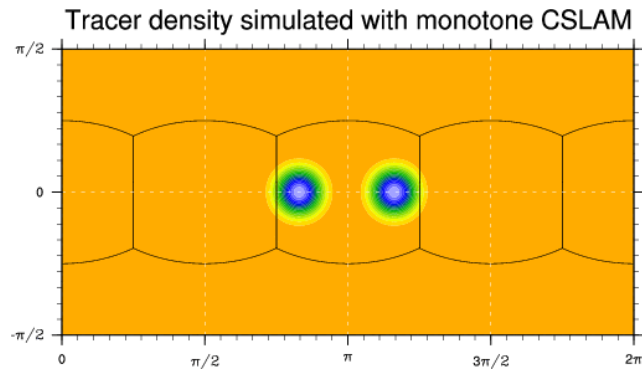
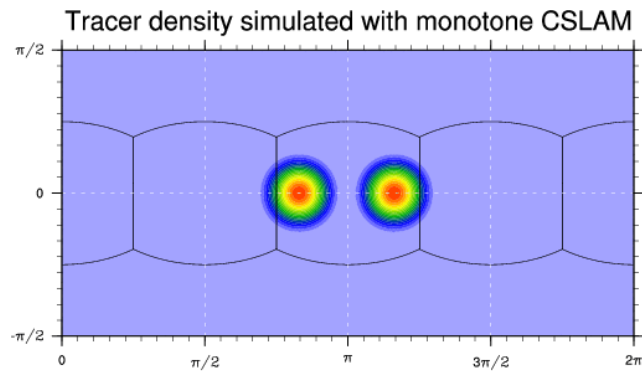
- a. Mixing that resembles `real' mixing – convex hull (red area)
- b. Everything else is spurious unmixing



Thuburn and McIntyre (1997, JGR)

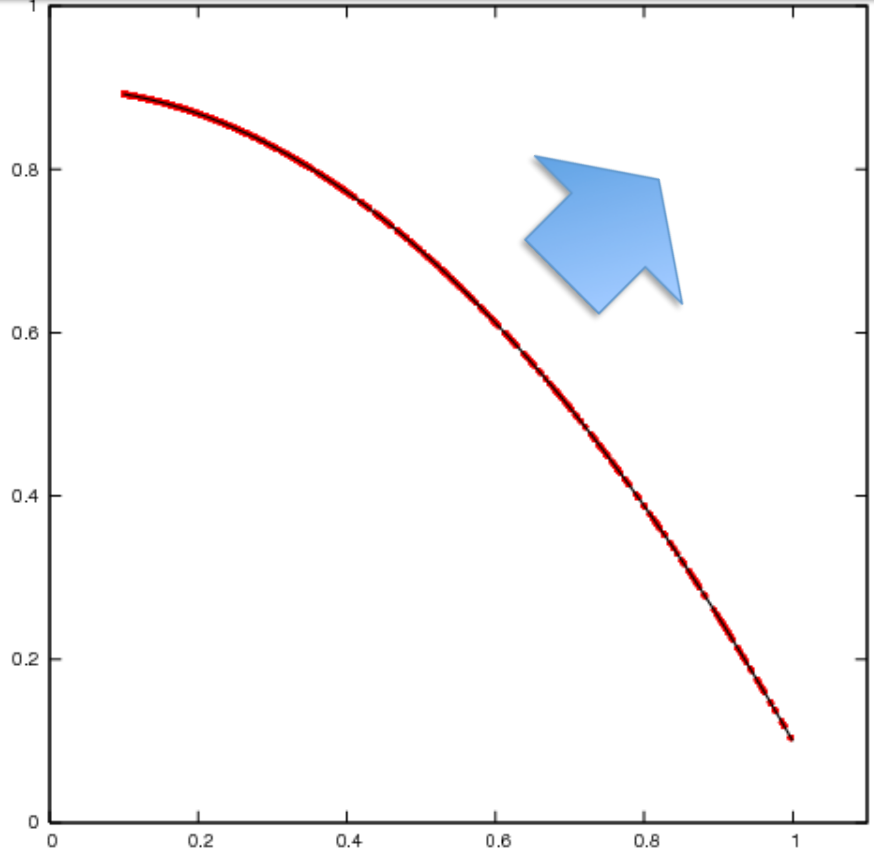
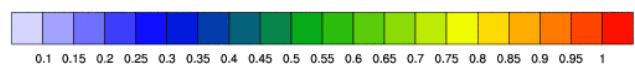
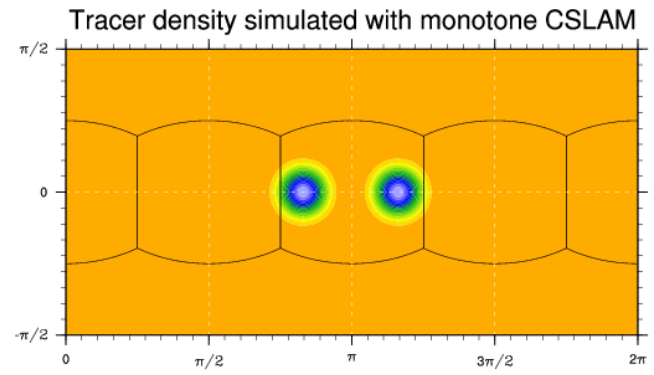
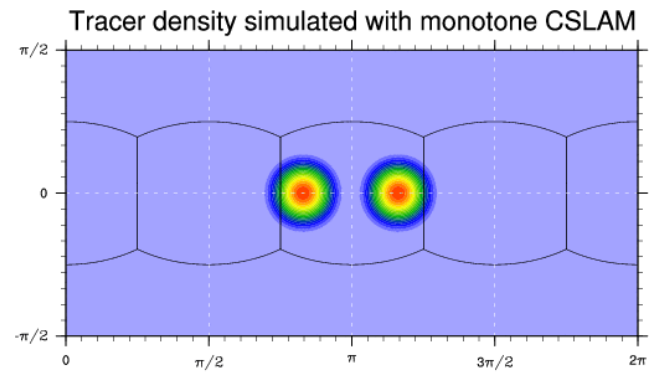
5. Preserving pre-existing functional relation between tracers under challenging flow conditions

Note: 1. **Max value decrease**, 2. Unmixing even if scheme is shape-preserving, 3. No expanding range unmixing



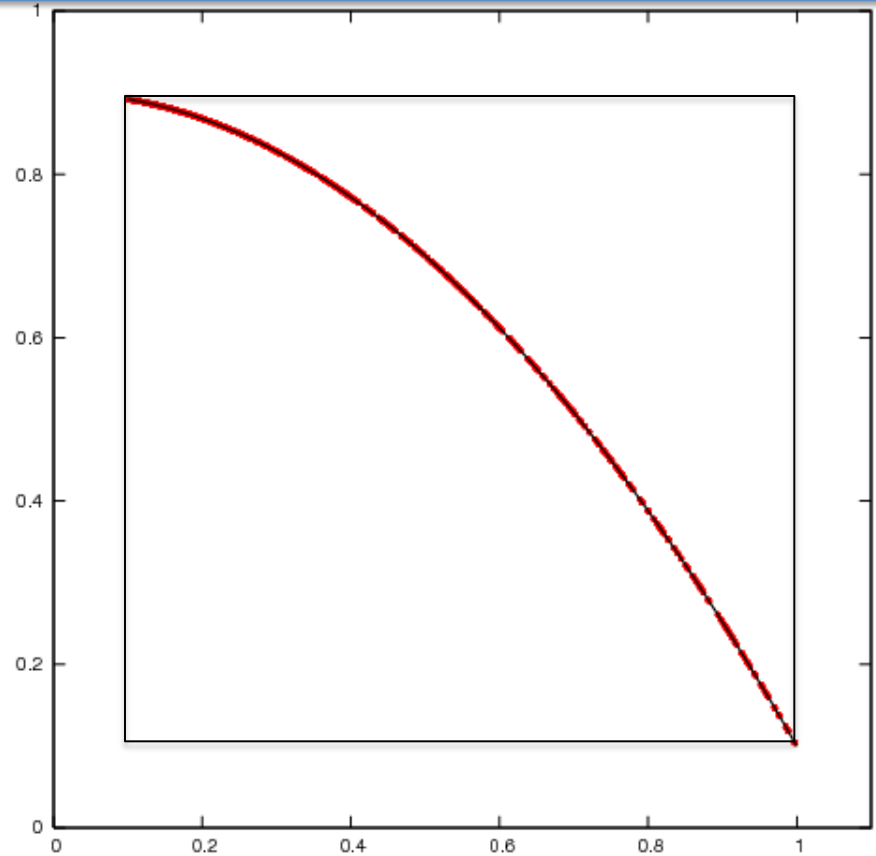
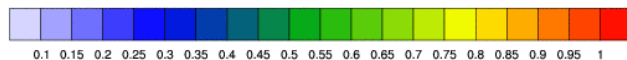
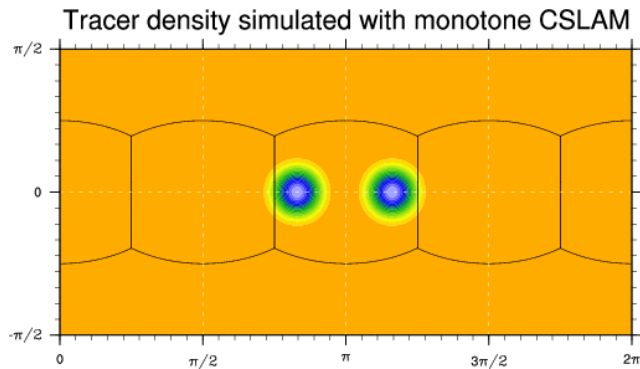
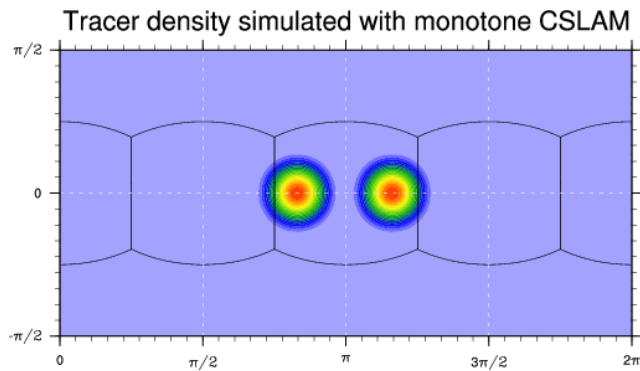
5. Preserving pre-existing functional relation between tracers under challenging flow conditions

Note: 1. Max value decrease, 2. **Unmixing even if scheme is shape-preserving**, 3. No expanding range unmixing

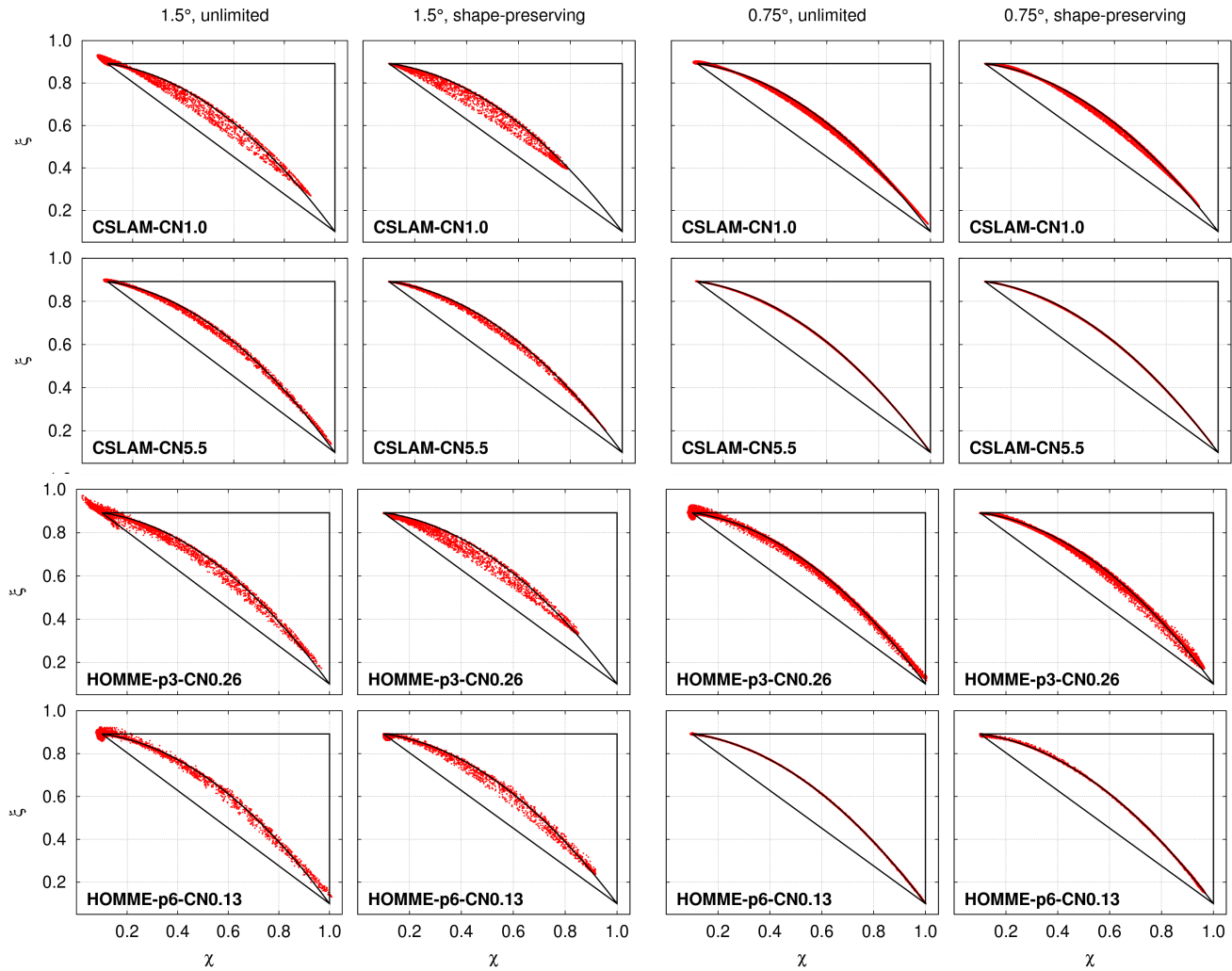


5. Preserving pre-existing functional relation between tracers under challenging flow conditions

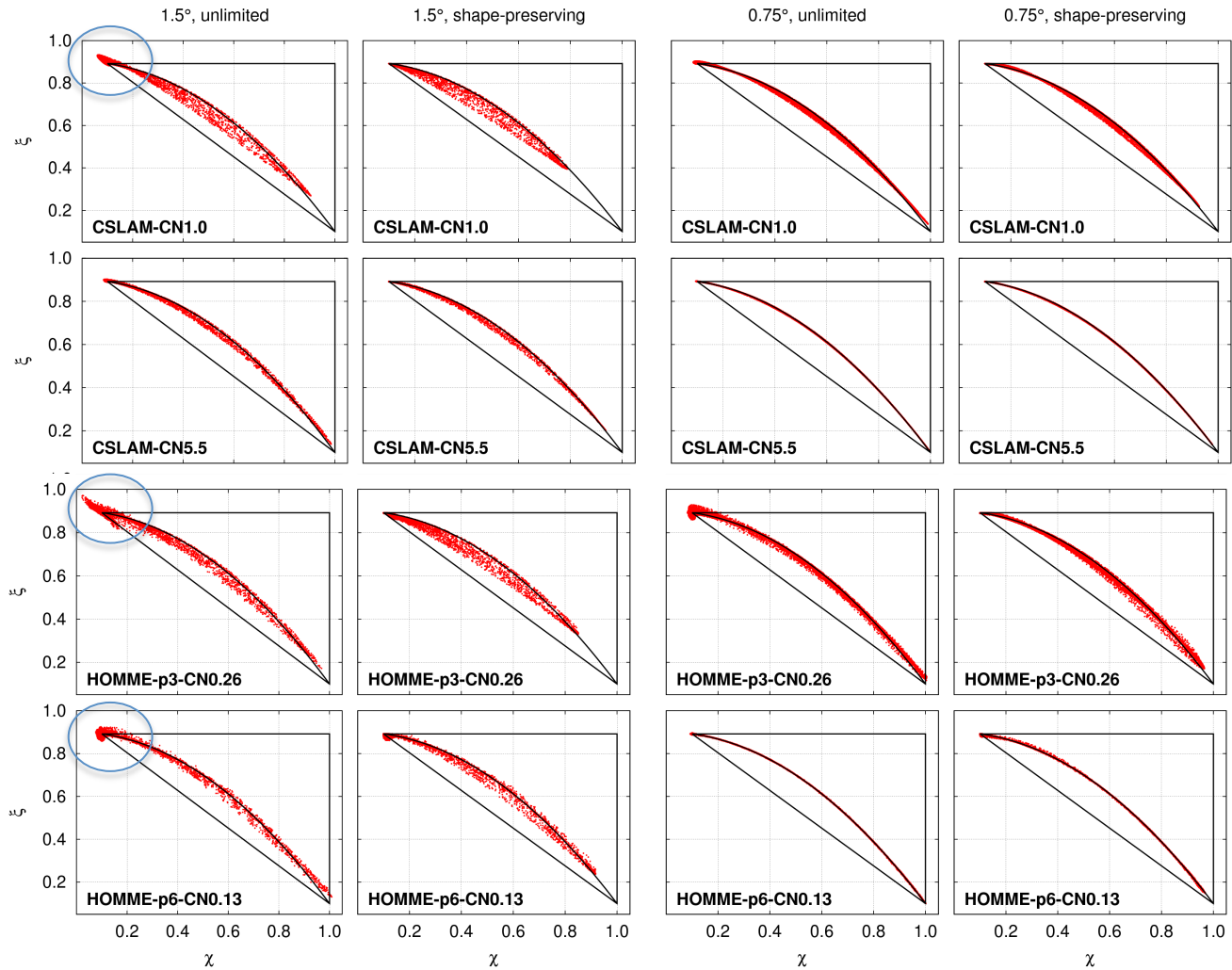
Note: 1. Max value decrease, 2. Unmixing even if scheme is shape-preserving, 3. **No expanding range unmixing**



Cubed-sphere models

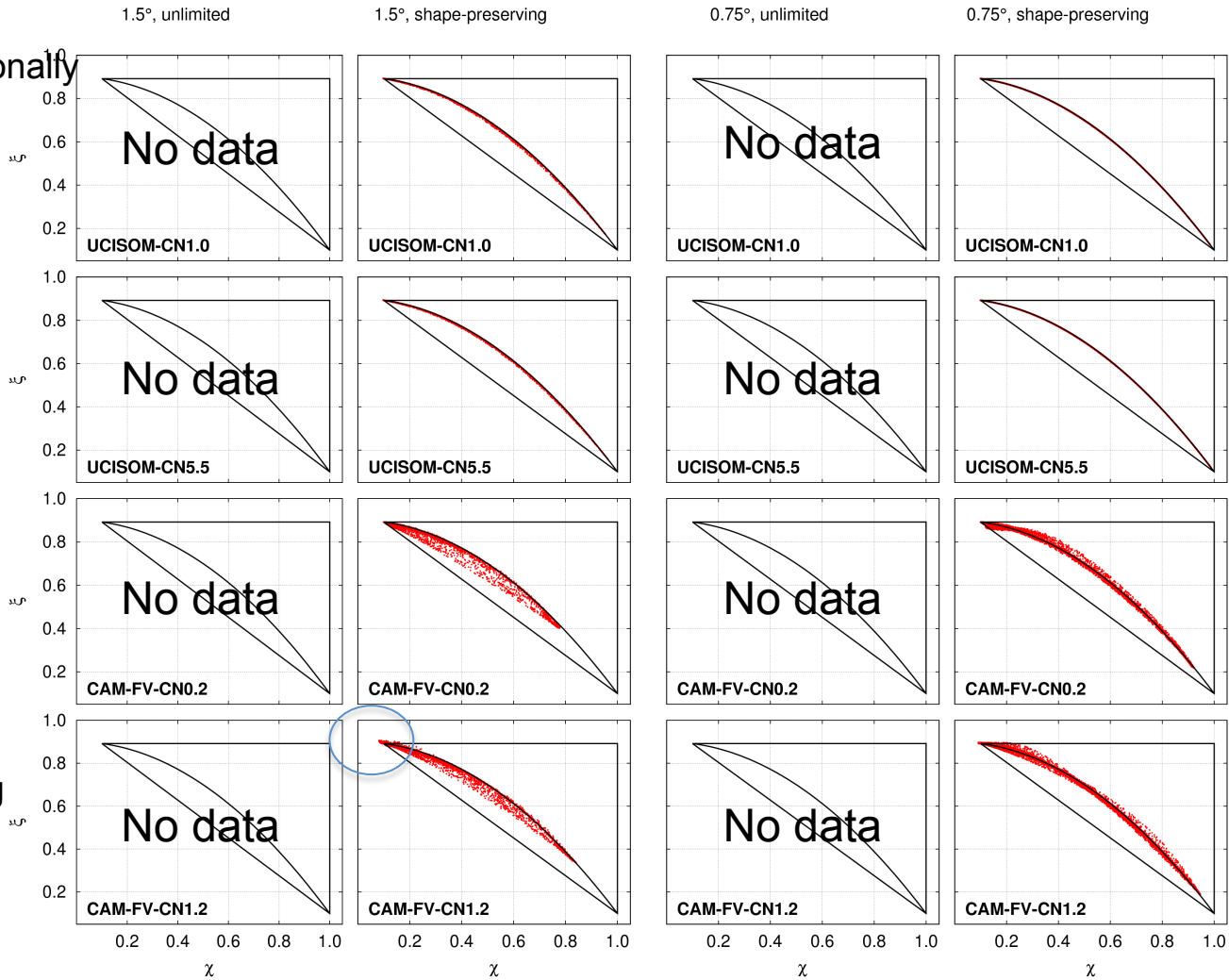


Cubed-sphere models



Reg. lat-lon models

Prather scheme performs exceptionally well



Shape-preserving scheme overshoots!

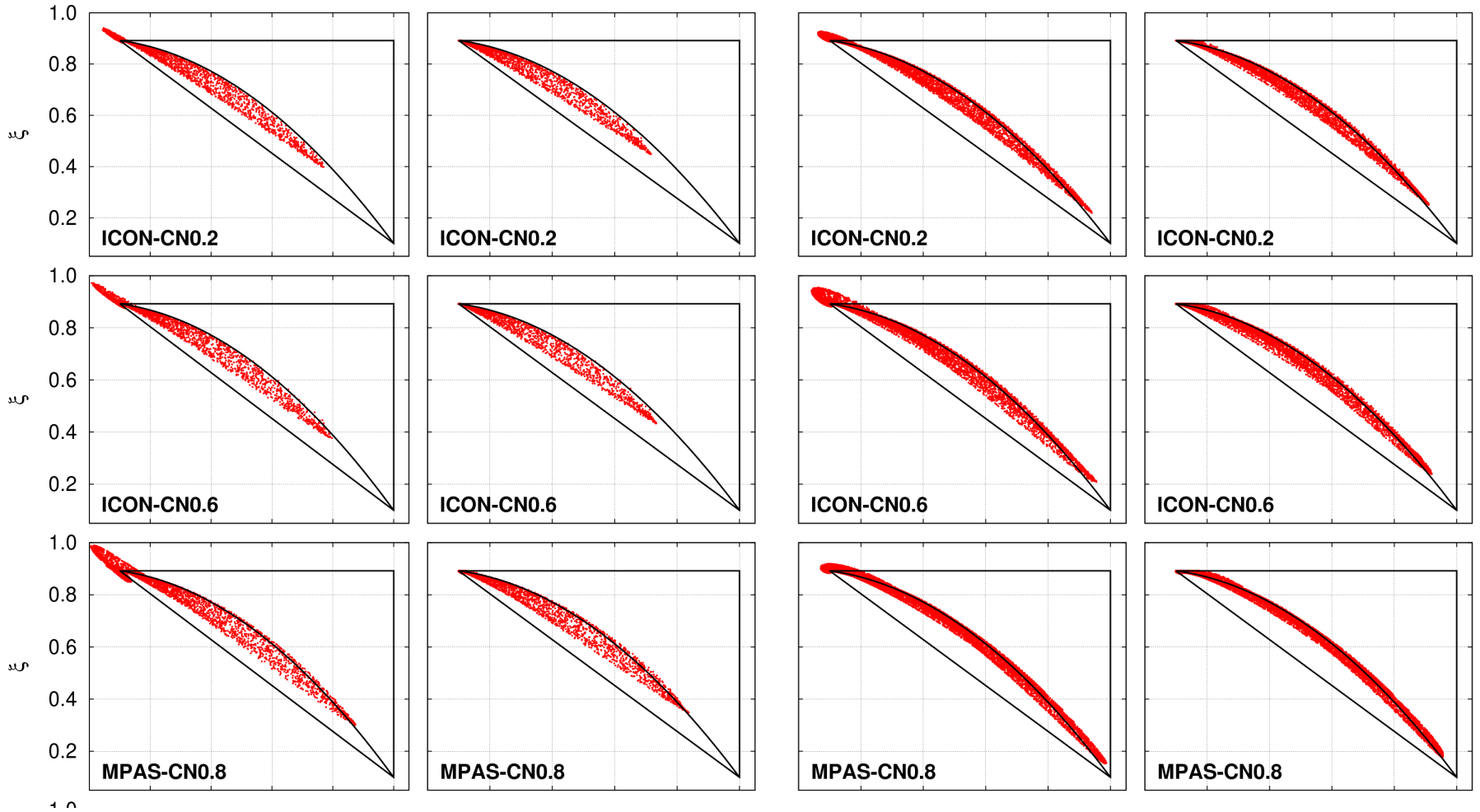
Icosahedral/Voronoi models

1.5°, unlimited

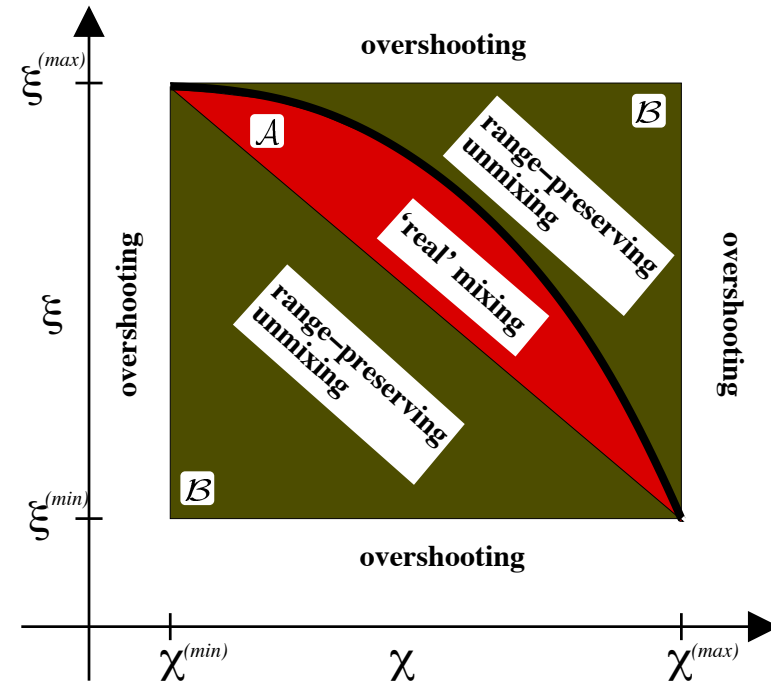
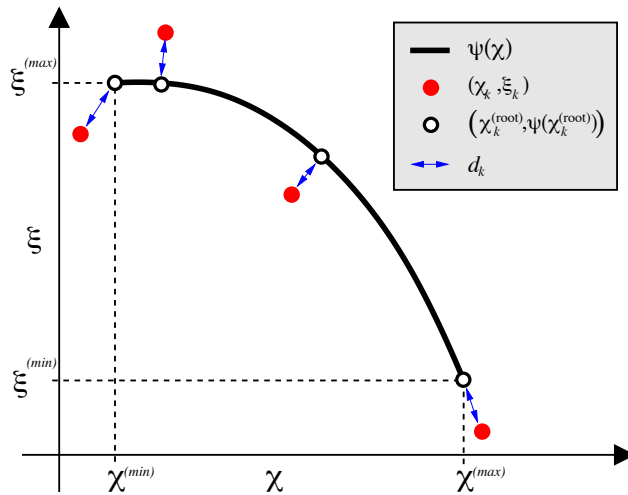
1.5°, shape-preserving

0.75°, unlimited

0.75°, shape-preserving



Quantifying mixing



$$\ell_r = \frac{1}{A} \sum_{k=1}^K \begin{cases} d_k \Delta A_k, & \text{if } (\chi_k, \xi_k) \in \mathcal{A}, \\ 0, & \text{else,} \end{cases} \quad (\text{C1})$$

where K is the total numbers of cells/points in the domain, ΔA_k is the spherical area of grid cell k and A is the total area of the domain, $A = \sum_{k=1}^K \Delta A_k$. The distance function d_k is the shortest normalized distance between the numerically computed scatter point (χ_k, ξ_k) and the preexisting functional curve within the range of the initial conditions.

This diagnostic does not rely on an analytical solution!

Lauritzen and Thuburn (2012, QJRMS)

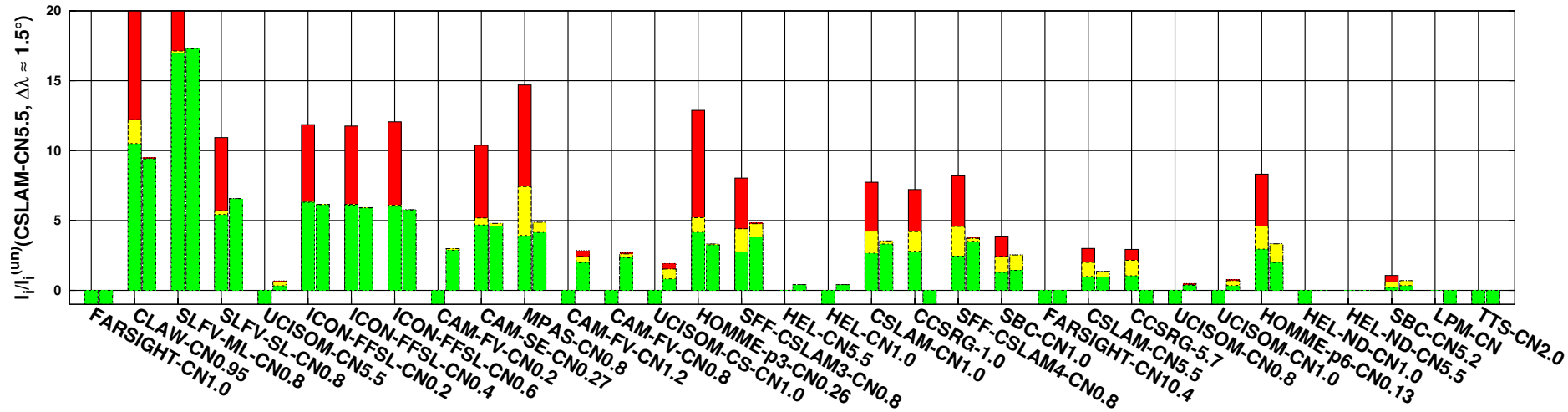


Quantifying mixing: stacked histogram (“real” mixing, range-preserving unmixing , overshooting)

For each scheme: left histogram is unlimited results; right is shape-preserving (sp)

Y-axis: Normalized by CSLAM unlimited mixing diagnostics at 1.5°

Mixing diagnostics at resolution $\Delta\lambda \approx 1.5^\circ$

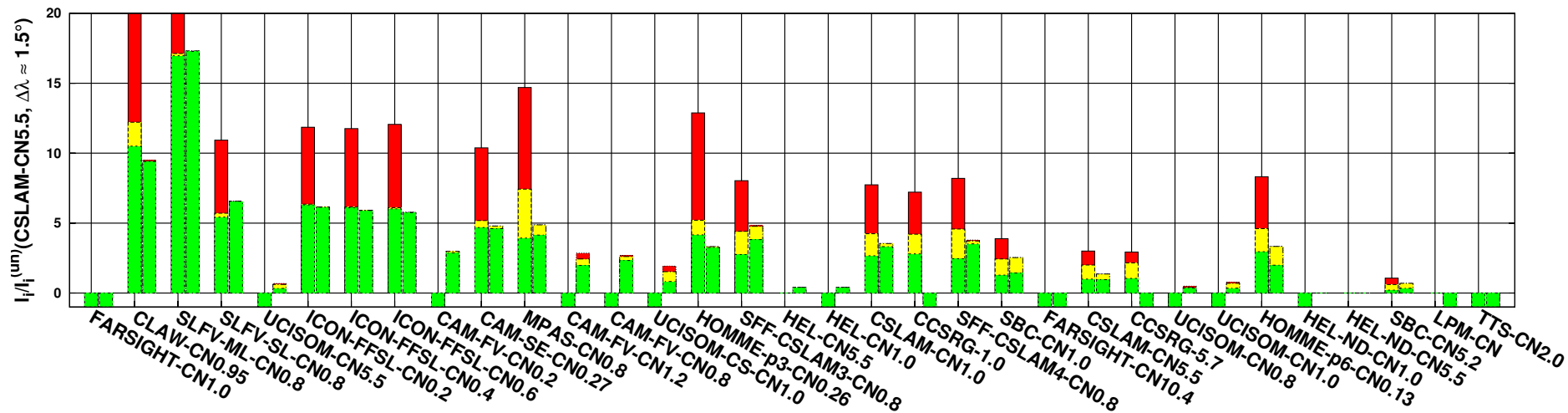


Quantifying mixing: stacked histogram (“real” mixing, range-preserving unmixing , overshooting)

For each scheme: left histogram is unlimited results; right is shape-preserving (sp)

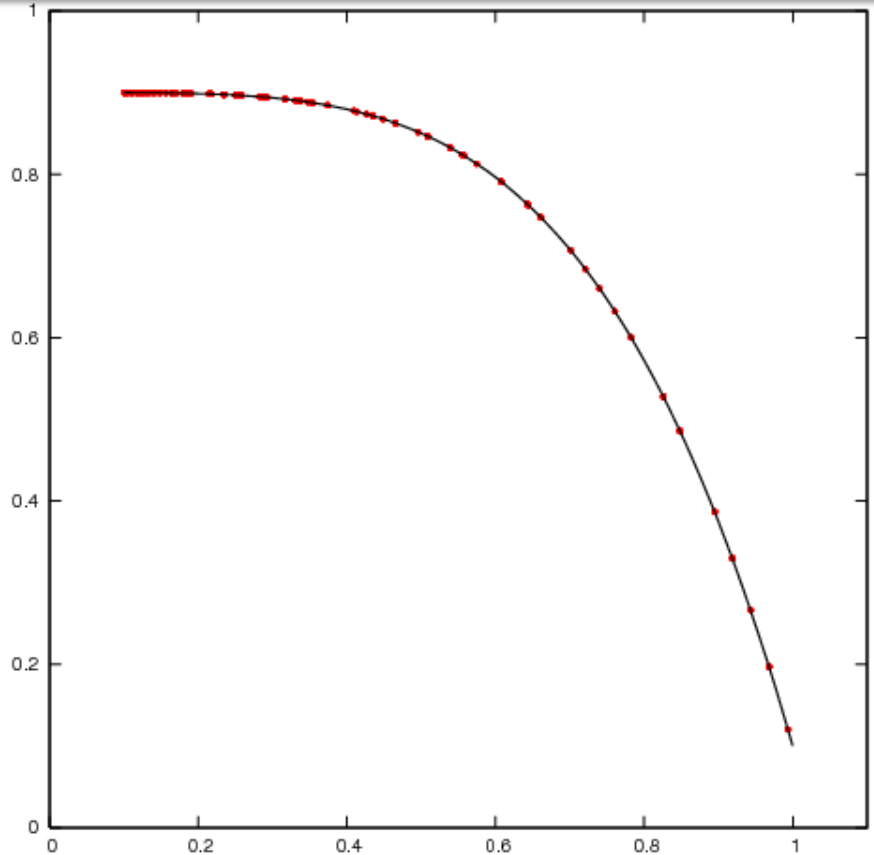
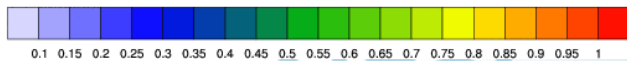
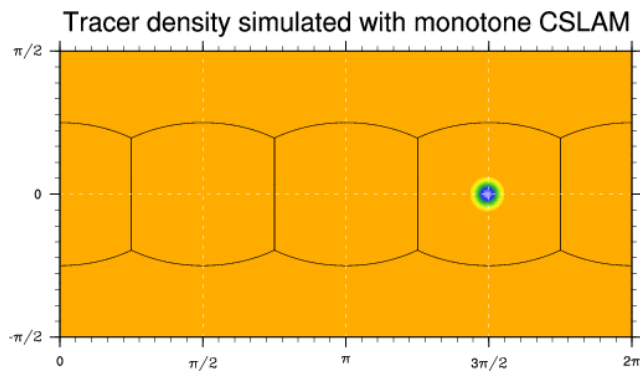
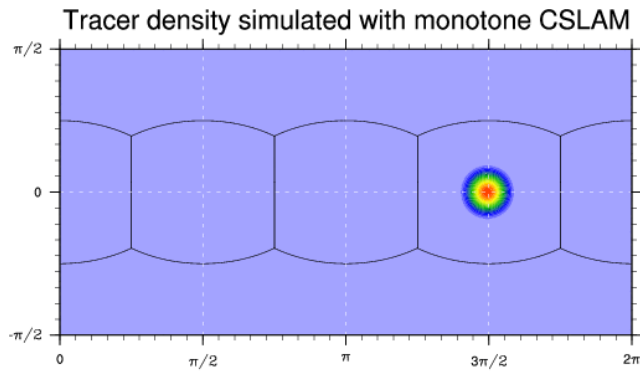
Y-axis: Normalized by CSLAM unlimited mixing diagnostics at 1.5°

Mixing diagnostics at resolution $\Delta\lambda \approx 1.5^\circ$

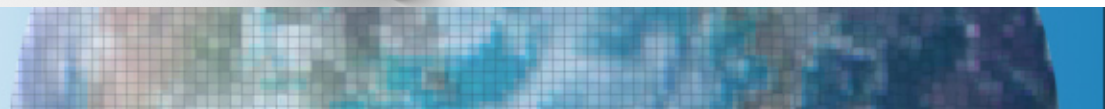


- If shape-preserving filter is “rigorous” red bars disappear: IMPORTANT!
- Yellow histograms reduce with sp filter: scheme produces results that are more physically realizable!
- For some schemes ‘real mixing’ decreases and for some it increases with sp filter.

It is key that tracer features collapse to smaller scales (as in nature)



This setup uses a 4th-order non-linear relation $\Psi(x) = ax^4 + b$



References

Harris, L.M., P.H. Lauritzen and R. Mittal, 2011: A Flux-form version of the Conservative Semi-Lagrangian Multi-tracer transport scheme (CSLAM) on the cubed sphere grid. *J. Comput. Phys.*: Vol. 230, Issue 4, pp. 1215–1237

Lauritzen, P.H., R.D. Nair and P.A. Ullrich, 2010: A conservative semi-Lagrangian multi-tracer transport scheme (CSLAM) on the cubed-sphere grid. *J. Comput. Phys.*: Vol. 229, Issue 5, pp. 1401–1424

Lauritzen, P.H., C. Erath and R. Mittal, 2011: On simplifying 'incremental remap'-type transport schemes. *J. Comput. Phys.*: Vol. 230, pp. 7957–7963.

Lauritzen, P.H., W.C. Skamarock, M.J. Prather and M.A. Taylor, 2012: A standard test case suite for two-dimensional linear transport on the sphere. *Geosci. Model Dev.*, Vol. 5, pp. 887-901

Lauritzen P.H. and J. Thuburn, 2012: Evaluating advection/transport schemes using interrelated Tracers, scatter plots and numerical mixing diagnostics. *Quart. J. Roy. Meteor. Soc.*: Vol. 138, pp. 906–918

Thuburn J., M.E. McIntyre, 1997. Numerical advection schemes, cross-isentropic random walks, and correlations between chemical species. *J. Geophys. Res.* 120(D6): 6775–6797